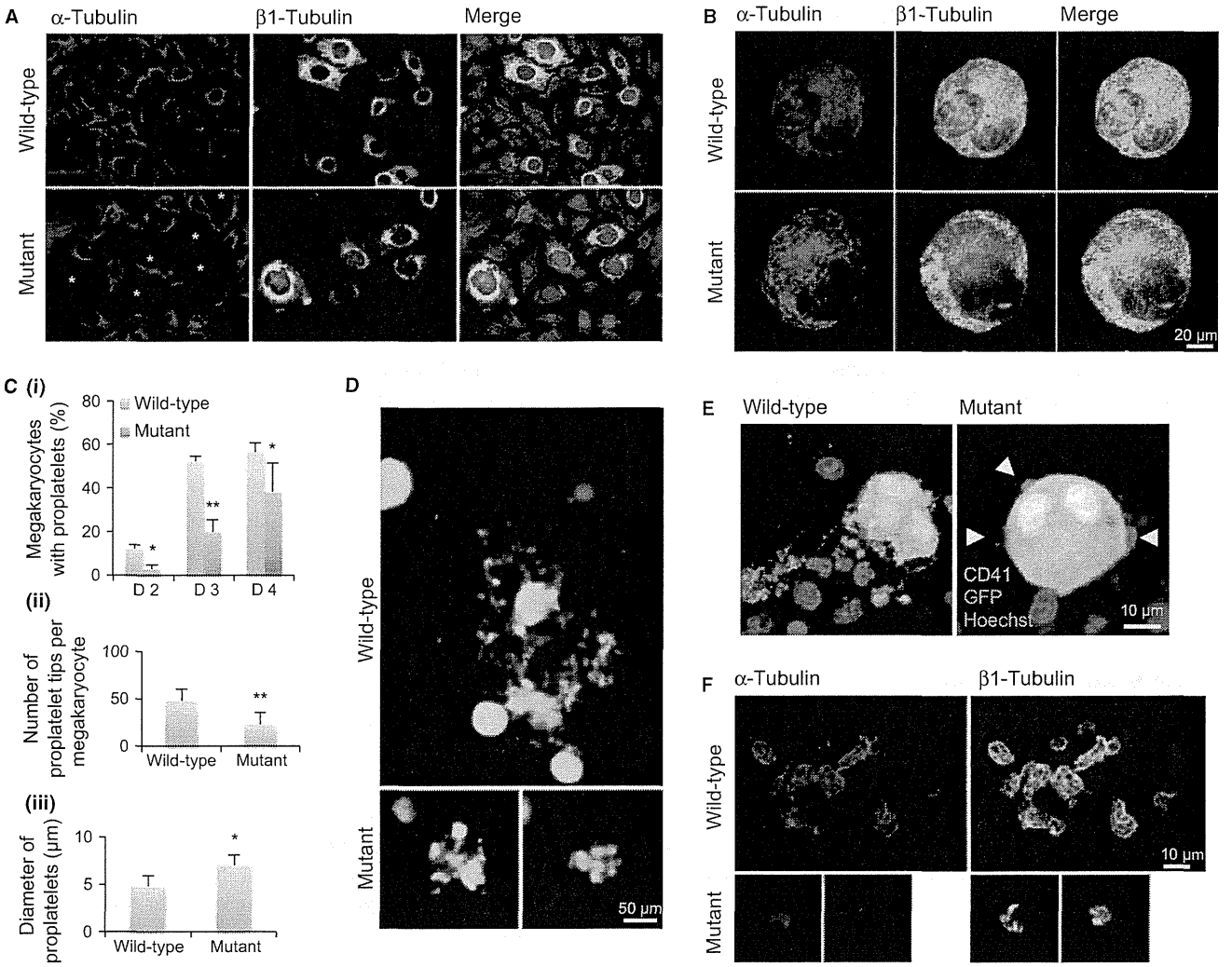

Figure 2 β1-tubulin transduction in Chinese hamster ovary (CHO) cells and mouse fetal liver-derived megakaryocytes. (A) β1-tubulin localization in CHO cells that were transiently transfected with pcDNA3.1/*TUBB1*myc. Cells were stained with antibodies to endogenous α-tubulin (red) and to the transfected β1-tubulin (green) as well as DAPI to label the DNA (blue). In merged images, CHO cells expressing wild-type β1-tubulin appear as yellow or orange, whereas cells expressing mutant β1-tubulin appear green because the expression of endogenous α-tubulin was decreased (asterisks). Cells are representative of five independent experiments. (B) Microtubule organization in β1-tubulin-transduced megakaryocytes. Cells were stained endogenous α-tubulin with DM1A (red) and the transduced β1-tubulin with anti-myc antibody (MBL, Nagoya, Japan) (green). Wild-type β1-tubulin was incorporated into microtubules, but mutant β1-tubulin was not. (C) Abnormal proplatelet formation in β1-tubulin-transduced megakaryocytes. (i) The percentage of megakaryocytes extending proplatelets was decreased in mutant-transduced cells. For each sample, 100 megakaryocytes were evaluated. (ii) The number of proplatelet tips per megakaryocyte was decreased in mutant-transduced cells. Fifty megakaryocytes per sample were evaluated. (iii) Size of proplatelet tips was increased in mutant-transduced cells. One hundred EGFP and β1-tubulin double-positive proplatelet tips per sample were evaluated. Data were analyzed using unpaired, two-tailed t-tests. $P < 0.05$ was considered statistically significant. Data are presented as mean ± SD. $*P < 0.05$, $**P < 0.001$. (D) Representative megakaryocytes extending proplatelets from three independent experiments. Fewer proplatelet tips/bulbous structures are evident, and size of tips is increased in megakaryocytes transduced with mutant. (E) Representative megakaryocytes from three independent live-cell imaging experiments. Megakaryocytes were differentiated from fetal liver cells of CAG-eGFP mice; therefore, the cytoplasm can be identified by eGFP signals (green). The cells were stained with Hoechst to identify nucleus (blue) and anti-CD41 antibody (red). Proplatelet elaboration is rare, and occasional large bleb protrusions are evident in megakaryocytes transduced with mutant (arrow heads). Original videos are available as Video S1 and S2. (F) Microtubule organization in proplatelet tips. Megakaryocyte cultures were cytospun on glass slides. Representative images from three independent experiments.

transcriptionally and translationally maintained for proper heterodimer assembly in cells, and when exogenous β-tubulin is overexpressed, the synthesis of the endogenous β-tubulin is inhibited and that of α-tubulin is upregulated (18, 19). The synthesis of β2- and β5-tubulins was increased in *TUBB1*-knockout mice (9). In contrast, α-tubulin was

disproportionally decreased relative to the decrease in β1-tubulin (Fig. 1B,D), and furthermore, β5-tubulin was substantially absent in our patients' platelets (data not shown). Defective mutant β1-tubulin would cause deregulated microtubule organization, as shown in platelets, CHO cells, and cultured megakaryocytes and proplatelet tips (Figs 1B and 2A,B,F). Thus, the deficient functional microtubules might lead to defective proplatelet formation and abnormal protrusion-like platelet release (Fig. 2D,E, Video S2). Defective microtubule organization and proplatelet formation were recently documented in Rac1- and Cdc42-deficient mice (20). Combined, these observations support the hypothesis that imbalanced transport of unpolymerized tubulins into platelets by proplatelet-independent platelet formation is related to the disorganization of microtubule-like structures in platelets.

Because p.D249N and p.R318W, locating at or near the interface, also reportedly cause macrothrombocytopenia in dogs and humans, respectively, mutations disrupting the structure of the intradimer interface might affect platelet morphology (10, 21). Analysis of congenital macrothrombocytopenia caused by tubulin mutations provides insights into the molecular mechanisms of platelet production and morphology.

Acknowledgements

The authors would like to thank R.C. Mulligan for 293gp and 293gpg cells, M. Onodera for pGCDNsamIRES/EGFP, M. Otsu for help with retroviral experiments, as well as Y. Kito-Takagi, M. Tajima, C. Yoshinaga, and T. Hirabayashi for technical assistance. This work was supported by grants from the Japan Society for the Promotion of Science KAKENHI (S.K.), Mitsubishi Pharma Research Foundation (S.K.), the 24th General Assembly of the Japanese Association of Medical Sciences (S.K.), Funding Program for Next Generation World-Leading Researchers (S.N.), and the Translational Systems Biology, Medicine Initiative (S.N.) from the Japan Science and Technology Agency.

Authorship and disclosures

S.K. designed and performed research, analyzed data, and wrote the paper; S.N. performed live-cell imaging experiments; H. Suzuki performed electron microscopic analysis; M.I. contributed patient samples; H. Saito supervised the research. The authors report no potential conflict of interests.

References

1. Balduini CL, Savoia A. Genetics of familial forms of thrombocytopenia. *Hum Genet* 2012;**131**:1821–32.
2. Kunishima S, Saito H. Congenital macrothrombocytopenias. *Blood Rev* 2006;**20**:111–21.
3. Nurden AT, Freson K, Seligsohn U. Inherited platelet disorders. *Haemophilia* 2012;**18**(Suppl 4):154–60.
4. Thon JN, Italiano JE Jr. Does size matter in platelet production? *Blood* 2012;**120**:1552–61.
5. Thon JN, Macleod H, Begonja AJ, Zhu J, Lee KC, Mogilner A, Hartwig JH, Italiano JE Jr. Microtubule and cortical forces determine platelet size during vascular platelet production. *Nat Commun* 2012;**3**:852.
6. Italiano JE Jr, Lecine P, Shivdasani RA, Hartwig JH. Blood platelets are assembled principally at the ends of proplatelet processes produced by differentiated megakaryocytes. *J Cell Biol* 1999;**147**:1299–312.
7. Thon JN, Montalvo A, Patel-Hett S, Devine MT, Richardson JL, Ehrlicher A, Larson MK, Hoffmeister K, Hartwig JH, Italiano JE Jr. Cytoskeletal mechanics of proplatelet maturation and platelet release. *J Cell Biol* 2010;**191**:861–74.
8. Lecine P, Italiano JE Jr, Kim SW, Villeval JL, Shivdasani RA. Hematopoietic-specific β1 tubulin participates in a pathway of platelet biogenesis dependent on the transcription factor NF-E2. *Blood* 2000;**96**:1366–73.
9. Schwer HD, Lecine P, Tiwari S, Italiano JE Jr, Hartwig JH, Shivdasani RA. A lineage-restricted and divergent β-tubulin isoform is essential for the biogenesis, structure and function of blood platelets. *Curr Biol* 2001;**11**:579–86.
10. Kunishima S, Kobayashi R, Itoh TJ, Hamaguchi M, Saito H. Mutation of the β1-tubulin gene associated with congenital macrothrombocytopenia affecting microtubule assembly. *Blood* 2009;**113**:458–61.
11. Kunishima S, Kashiwagi H, Otsu M, *et al.* Heterozygous ITGA2B R995W mutation inducing constitutive activation of the αIIbβ3 receptor affects proplatelet formation and causes congenital macrothrombocytopenia. *Blood* 2011;**117**:5479–84.
12. Suzuki H, Kaneko T, Sakamoto T, Nakagawa M, Miyamoto T, Yamada M, Tanoue K. Redistribution of α-granule membrane glycoprotein IIb/IIIa (integrin αIIbβ3) to the surface membrane of human platelets during the release reaction. *J Electron Microscopy* 1994;**43**:282–9.
13. White JG, Krumwiede M. Isolation of microtubule coils from normal human platelets. *Blood* 1985;**65**:1028–32.
14. Kunishima S, Okuno Y, Yoshida K, *et al.* ACTN1 mutations cause congenital macrothrombocytopenia. *Am J Hum Genet* 2013;**92**:431–8.
15. Lowe J, Li H, Downing KH, Nogales E. Refined structure of αβ-tubulin at 3.5 a resolution. *J Mol Biol* 2001;**313**:1045–57.
16. Yang H, Ganguly A, Yin S, Cabral F. Megakaryocyte lineage-specific class VI β-tubulin suppresses microtubule dynamics, fragments microtubules, and blocks cell division. *Cytoskeleton* 2011;**68**:175–87.
17. Patel-Hett S, Richardson JL, Schulze H, *et al.* Visualization of microtubule growth in living platelets reveals a dynamic marginal band with multiple microtubules. *Blood* 2008;**111**:4605–16.
18. Cleveland DW. Autoregulated instability of tubulin mRNAs: a novel eukaryotic regulatory mechanism. *Trends Biochem Sci* 1988;**13**:339–43.

19. Gonzalez-Garay ML, Cabral F. Overexpression of an epitope-tagged β-tubulin in Chinese hamster ovary cells causes an increase in endogenous alpha-tubulin synthesis. *Cell Motil Cytoskeleton* 1995;**31**:259–72.
20. Pleines I, Dutting S, Cherpokova D, *et al.* Defective tubulin organization and proplatelet formation in murine megakaryocytes lacking Rac1 and Cdc42. *Blood* 2013;**122**:3178–87.
21. Davis B, Toivio-Kinnucan M, Schuller S, Boudreaux MK. Mutation in β1-tubulin correlates with macrothrombocytopenia in Cavalier King Charles Spaniels. *J Vet Intern Med* 2008;**22**:540–5.

Supporting Information

Additional Supporting Information may be found in the online version of this article:

Video S1. Live-cell imaging of platelet release. Original movie of Figure 2E (left, wild type).

Video S2. Live-cell imaging of platelet release. Original movie of Figure 2E (right, mutant).

GATA2 regulates differentiation of bone marrow-derived mesenchymal stem cells

Mayumi Kamata,[1] Yoko Okitsu,[1] Tohru Fujiwara,[1,2] Masahiko Kanehira,[1] Shinji Nakajima,[1] Taro Takahashi,[1] Ai Inoue,[1] Noriko Fukuhara,[1] Yasushi Onishi,[1] Kenichi Ishizawa,[1] Ritsuko Shimizu,[3] Masayuki Yamamoto,[4] and Hideo Harigae[1,2]

[1]Departments of Hematology and Rheumatology; [2]Molecular Hematology/Oncology; [3]Molecular Hematology; and [4]Medical Biochemistry, Tohoku University Graduate School of Medicine, Sendai, Japan

ABSTRACT

The bone marrow microenvironment comprises multiple cell niches derived from bone marrow mesenchymal stem cells. However, the molecular mechanism of bone marrow mesenchymal stem cell differentiation is poorly understood. The transcription factor GATA2 is indispensable for hematopoietic stem cell function as well as other hematopoietic lineages, suggesting that it may maintain bone marrow mesenchymal stem cells in an immature state and also contribute to their differentiation. To explore this possibility, we established bone marrow mesenchymal stem cells from GATA2 conditional knockout mice. Differentiation of GATA2-deficient bone marrow mesenchymal stem cells into adipocytes induced accelerated oil-drop formation. Further, GATA2 loss- and gain-of-function analyses based on human bone marrow mesenchymal stem cells confirmed that decreased and increased GATA2 expression accelerated and suppressed bone marrow mesenchymal stem cell differentiation to adipocytes, respectively. Microarray analysis of GATA2 knockdowned human bone marrow mesenchymal stem cells revealed that 90 and 189 genes were upregulated or downregulated by a factor of 2, respectively. Moreover, gene ontology analysis revealed significant enrichment of genes involved in cell cycle regulation, and the number of G1/G0 cells increased after GATA2 knockdown. Concomitantly, cell proliferation was decreased by GATA2 knockdown. When GATA2 knockdowned bone marrow mesenchymal stem cells as well as adipocytes were co-cultured with CD34-positive cells, hematopoietic stem cell frequency and colony formation decreased. We confirmed the existence of pathological signals that decrease and increase hematopoietic cell and adipocyte numbers, respectively, characteristic of aplastic anemia, and that suppress GATA2 expression in hematopoietic stem cells and bone marrow mesenchymal stem cells.

Introduction

Bone marrow mesenchymal stem cells (BM-MSC) are self-renewing precursor cells that differentiate into bone, fat, cartilage, and stromal cells of the bone marrow, thereby forming a microenvironment that maintains hematopoietic stem cells.[1] Accumulating evidence indicates the importance of the bone marrow microenvironment during hematopoietic cell development. Increased adipogenesis in the bone marrow negatively affects hematopoietic activity,[2,3] whereas the osteoblastic niche supports hematopoietic stem cell function by activating Notch signaling.[4] Therefore, precise regulation of BM-MSC differentiation into various lineages maintains hematopoiesis.

Preadipocytes derived from MSC mature into adipocytes through a complex process involving numerous extracellular factors as well as transcription factors.[1,5] Studies conducted on preadipocyte cell lines, such as mouse 3T3-L1 and 3T3-F442A, have uncovered the CCAAT/enhancer binding protein (C/EBP) family of transcription factors and the peroxisome proliferator-activated receptor γ (PPARγ) as key proadipogenic regulators.[6,7] During preadipocyte–adipocyte differentiation, the expression of C/EBPβ and C/EBPδ initially increases, which subsequently activates the expression of C/EBPα and PPARγ, leading to the induction of genes involved in adipocyte function.[8,9] However, the mechanism of differentiation of BM-MSC into adipogenic progenitors and ultimately into mature adipocytes in the bone marrow remains to be elucidated.

GATA2, a transcription factor critically required in the genesis and/or function of hematopoietic stem cells (HSC),[10-13] is expressed in various hematopoietic and non-hematopoietic tissues, including HSC, multipotent hematopoietic progenitors, erythroid precursors, megakaryocytes, eosinophils, mast cells, endothelial cells, and specific neurons.[11,12,14-16] GATA2 is expressed by preadipocytes and BM-MSC and plays a central role in the control of adipogenesis.[13,16,17] GATA2 overexpression in a mouse preadipocytic stromal cell line induces resistance to adipocyte differentiation, whereas GATA2 knockdown accelerates adipocyte differentiation,[17] implying that GATA2 functions to arrest preadipocyte differentiation. Although GATA2 may suppress transcription of *C/EBP* and *PPARγ* in preadipocytes,[16,18] the molecular mechanism by which GATA2 controls adipocyte differentiation remains unclear.

Aplastic anemia is characterized by decreased HSC and fatty marrow replacement. Moreover, GATA2 expression is decreased in CD34-positive cells in aplastic anemia,[19,20] Because BM-MSC express GATA2, it is possible that the signal that downregulates GATA2 expression in HSC may also suppress its expression in BM-MSC in aplastic anemia, thereby resulting in fewer HSC and an impaired microenvironment, which could support hematopoiesis. To test this hypothesis, we assessed the role of GATA2 during differentiation from BM-MSC.

 doi:10.3324/haematol.2014.105692
The online version of this article has a Supplementary Appendix.
Manuscript received on February 12, 2014. Manuscript accepted on August 7, 2014.
Correspondence: harigae@med.tohoku.ac.jp

Methods

Generation of bone marrow mesenchymal stem cells

To generate mouse BM-MSC, bone marrow cells from GATA2 conditional knockout mice were cultured in MesenCult MSC Basal Medium supplemented with 20% MSC stimulatory supplements (Stem Cell Technologies). The BM-MSC were transfected with the retroviruses expressing iCre to delete the DNA binding domain of GATA2 by inducing the Cre-loxP system.[21,22]

To generate human BM-MSC, bone marrow mononuclear cells from healthy donors were cultured with Dulbecco's modified Eagle's medium (Life Technologies) supplemented with 20% fetal bovine serum (Life Technologies), 10 ng/mL basic fibroblast growth factor (PeproTech), 10 mM HEPES (Life Technologies), and 100 μg/mL penicillin/streptomycin (Invitrogen).[23-25] Established BM-MSC were used until the seventh generation.

The study was approved by the ethical committee of Tohoku University Graduate School of Medicine. Clinical samples were collected after obtaining written informed consent. The ethics policies of the Declaration of Helsinki were followed.

Characterization of bone marrow mesenchymal stem cells

BM-MSC immunophenotypes were determined using a FACSAria II (BD). To induce differentiation into adipocytes, human Mesenchymal Stem Cell Adipogenic Differentiation Medium (Lonza) was used. After 12–16 days, morphological changes were assessed using an inverted microscope. Typical adipocytes were stained with Oil Red O.[2] The area of mature adipocytes was determined using HistoQuest software (Novel Science).

Quantitative reverse transcriptase polymerase chain reaction analysis and transcription profiling

Quantitative reverse transcriptase polymerase chain reaction analysis (RT-PCR) was performed as previously described.[26] Primer sequences are available upon request.

For transcription profiling, the Human Genome U133 Plus 2.0 Array was used (Affymetrix). Gene ontology analysis was conducted using the DAVID bioinformatics program (*http://david.abcc.ncifcrf.gov/*).

Short interfering RNA-mediated knockdown

Anti-GATA2 and control short interfering RNA (siRNA)[26] were transfected into human BM-MSC with Lipofectamine™ RNAiMAX reagent (Life Technologies). Cells were analyzed 48 h after transfection.

Viral vectors and cell transduction

Retroviral overexpression of GATA2 was performed using the MSCV retrovirus vector, which co-expresses green fluorescent protein (GFP) by internal ribosome entry sites (IRES), transfecting into Platinum Retroviral Packaging Cell Lines (PLAT-F)[27] with FuGENE HD (Roche). Human BM-MSC were pretreated with Retronectin (TAKARA BIO.), and GFP-positive cells were sorted using FACSAria II (BD Biosciences).

Co-culture of CD34-positive-enriched cells with a mesenchymal stem cell feeder layer

BM-MSC were transfected with control or GATA2-siRNA. On day 3, control and GATA2 knockdowned BM-MSC, respectively, were replaced with serum-free medium containing CD34-positive-enriched cells (RIKEN). Serum-free medium (StemPro-34 SFM: Life Technologies) contained 100 ng/mL stem cell factor, 100 ng/mL interleukin (IL)-3, and 25 ng/mL granulocyte-monocyte colony-stimulating factor (Peprotech). The cells were co-cultured for 7 days, and subsequently harvested and analyzed with FACSAria II (BD).

Colony-forming cell assay

CD34 positive-enriched cells, co-cultured with BM-MSC for 7 days, were seeded into semisolid culture (MethoCult™ H4435, Stem Cell Technologies). After 14 days, colony-forming units were counted.

Cell proliferation and cell cycle analysis

The total number of viable cells was determined by a colorimetric method using MTS (3-4,5-dimethylthiazol-2-yl-5-3-carboxymethoxyphenyl-2-4-sulfophenyl-2H-tetrazolium, inner salt; CellTiter 96). Absorbance at 490 nm was measured with an iMark microplate reader (Bio-rad). For cell cycle analysis, cells were fixed in ice-cold 70% ethanol and stained with 20 μg/mL propidium iodide (Sigma), 0.2 mg/mL RNase (Sigma), and 0.1% Triton X-100 (Sigma). DNA content was determined using FACSAria II and FlowJo software (*http://www.flowjo.com/*).

Statistical analysis

Statistical significance was assessed using a two-sided Student *t*-test.

Results

Acceleration of adipocyte differentiation in mesenchymal stem cells from GATA2 knockout mice

We first generated BM-MSC from bone marrow cells of conditional GATA2 knockout mice (GATA2^{fl}), in which the DNA binding domain of GATA2 (exon 5 encoding the C-terminal zinc-finger motif) could be deleted by inducing the Cre-loxP system (GATA2–) (*Online Supplementary Figure S1A*). We confirmed that GATA2^{fl} BM-MSC retained the potential to differentiate into adipogenic lineages (*Online Supplementary Figure S1B*). Flow cytometric analysis confirmed the characteristic immunophenotype,[28] showing that GATA2^{fl} BM-MSC expressed CD29, CD44 and Sca-1 but not markers such as CD11b, CD34 and CD45 (*Online Supplementary Figure S1C*).

To determine whether the loss of GATA2 influenced the BM-MSC phenotype, the DNA-binding domain of GATA2 was deleted using the Cre-loxP system, and GATA2 knockout–BM-MSC (GATA2$^-$ BM-MSC) were generated. Quantitative RT-PCR analysis revealed that *Gata2* expression was significantly decreased in the GATA2$^-$ MSC, implying that iCre-mediated deletion of the GATA2 C-finger resulted in decreased GATA2 autoregulation (Figure 1A). When GATA2^{fl} and GATA2– BM-MSC were exposed to adipogenic differentiation stimuli, we observed an overall increase in the expression of *Cebpa* (CEBPα), *Pparg* (PPARγ), and *Fabp4* (aP2) in GATA2$^-$ BM-MSC (Figure 1B). Moreover, the expression of these genes peaked during days 8–12 of differentiation and then dropped to levels similar to those of control cells (Figure 1B), whereas the expression level of *Cebpb* (CEBPβ) was slightly higher in GATA2$^-$ BM-MSC at the early (day 4) and last (day 16) stages of differentiation (Figure 1B). Furthermore, oil drop formation was markedly increased in GATA2$^-$ MSC (Figure 1C). These results suggest that loss of GATA2 function induces the expression of adipogenic factors and adipocyte differentiation of BM-MSC.

Generation and characterization of human bone marrow mesenchymal stem cells

Next, to elucidate the role of GATA2 in the context of

human BM-MSC differentiation, we generated BM-MSC from human mononuclear cells derived from bone marrow samples. We confirmed that BM-MSC differentiated into the adipogenic lineage (*Online Supplementary Figure S2A*). Flow cytometric analysis further confirmed the characteristic immunophenotype,[24,29,30] showing that the BM-MSC expressed CD29, CD44, CD90 and CD105 but not CD14, CD34, and CD45 (*Online Supplementary Figure S2B*).

Short interfering RNA-mediated GATA2 knockdown promotes differentiation of human bone marrow mesenchymal stem cells into adipocytes

To determine whether GATA2 regulates adipocyte differentiation in human BM-MSC, we suppressed GATA2 expression using a specific siRNA. Control or GATA2-siRNA were transfected into human BM-MSC 48 h before inducing adipocyte differentiation. We demonstrated that GATA2 mRNA levels were significantly decreased on day 0 and during adipocyte differentiation until day 8 (Figure 2A-B). Thereafter, we analyzed the expression of key adipocyte-specific genes at various time-points during adipocyte differentiation. The levels of expression of *C/EBPα, PPARγ* and *aP2* were significantly increased in the GATA2-knockdowned cells (Figure 2B). Furthermore, oil drop formation on day 12 was significantly increased in the GATA2 knockdown cells, as determined based on the Oil Red O staining-positive area (Figure 2C-D). These findings were consistent with the results for GATA2-deficient murine BM-MSC (Figure 1).

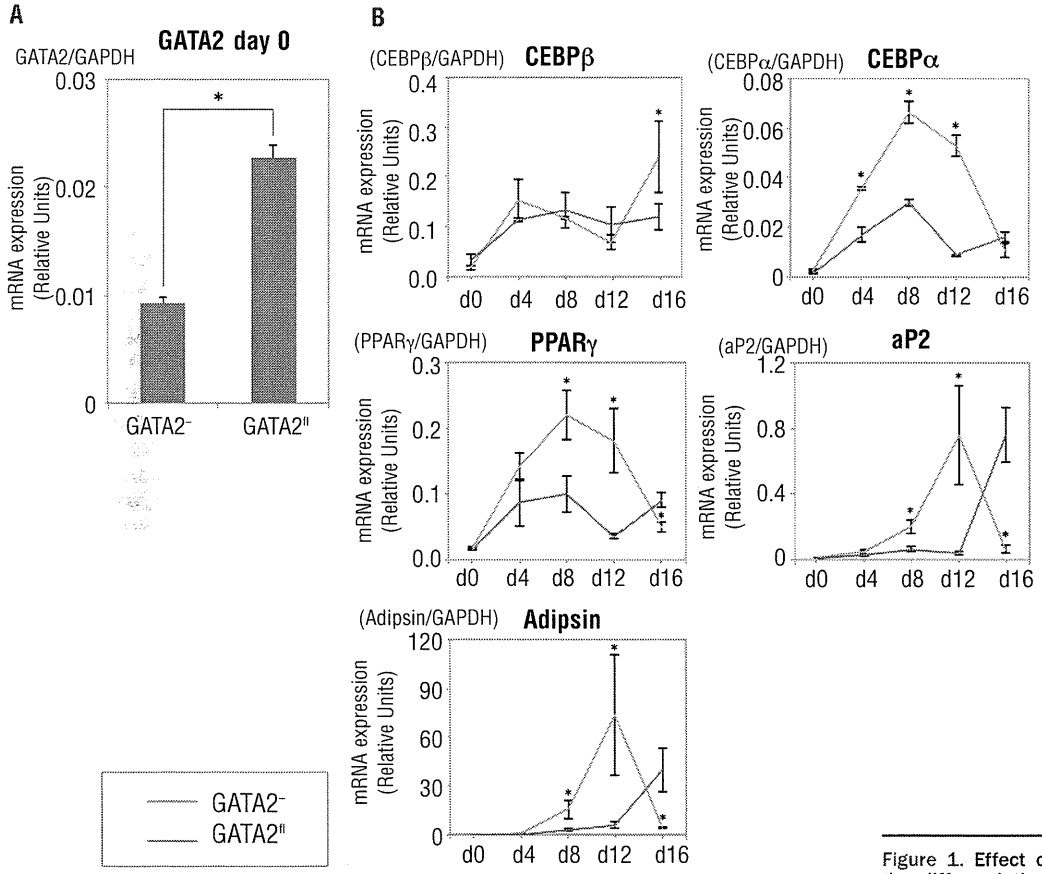

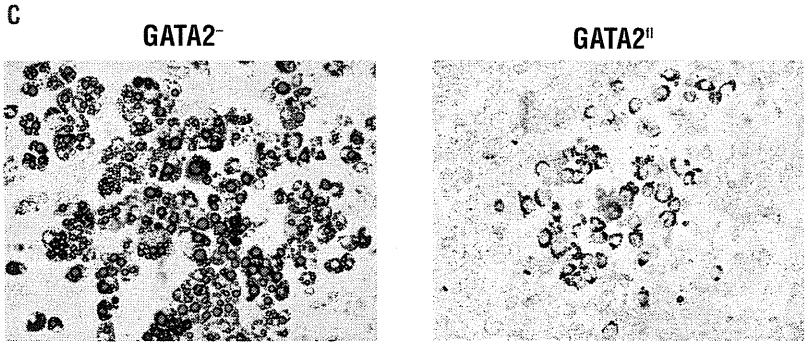

Figure 1. Effect of GATA2 depletion on the differentiation of murine MSC into adipocytes. GATA2-depleted BM-MSC (GATA2⁻) were generated by inducing iCre into the BM-MSC, established from GATA2 conditional knockout mice (GATA2fl). Each BM-MSC was then differentiated into the adipocyte lineage for up to 16 days. The data are representative of two independent BM-MSC lines. (A, B) Quantitative RT-PCR analysis for Gata2 expression on day 0 (A) and adipocyte-specific genes during adipocyte differentiation (B). The expression of each target gene relative to that of *Gapdh* was calculated. The data are expressed as mean ± standard deviation, SD (n = 3). *$P < 0.05$. (C) Oil Red O staining on day 16. The picture is a representative example of at least three independent experiments.

GATA2 overexpression suppresses differentiation of human bone marrow mesenchymal stem cells into adipocytes

We overexpressed GATA2 in human BM-MSC using MSCV-GFP-IRES. After transfecting GATA2-expressing or control retroviruses, GFP-positive cells were sorted. Quantitative RT-PCR assay confirmed GATA2 overexpression (Figure 3A, B). When these cells were differentiated into adipocytes, the levels of expression of *C/EBPα*, *PPARγ*, *aP2* and *Adipsin* were significantly diminished by GATA2 overexpression (Figure 3B). Concomitantly, oil drop formation on day 12 was also significantly decreased in cells overexpressing GATA2 (Figure 3C,D).

Taken together, our data suggest that decreased GATA2 expression by human BM-MSC accelerates adipocyte differentiation, whereas GATA2 overexpression suppresses adipocyte differentiation.

Enrichment of cell cycle regulatory genes based on transcriptional profiling to identify GATA2-regulated genes in human bone marrow mesenchymal stem cells

To identify GATA2-target genes in BM-MSC, we conducted comprehensive expression profiling of BM-MSC transfected with control or GATA2-siRNA. Inhibition of *GATA2* expression was confirmed based on the profiling data as well as quantitative RT-PCR analysis (0.000104 ± 0.000008 and 0.000198 ± 0.000022, for GATA2 siRNA and control siRNA, respectively, $P<0.05$) (Table 1, *Online Supplementary Table S1*, *Online Supplementary Figure S3*). Based on the average of two independent datasets, we demonstrated that GATA2 knockdown activated and repressed 90 and 189 genes (> 2-fold), respectively (Table 1, *Online Supplementary Table S1*). The analysis revealed the differential expression of cell-cycle regulators (*CHEK1*, *CCNB1*, *CCNB2*, *GTSE1*, and *CDC20*), adhesion molecules (*LAMP1* and *CD44*), as well as

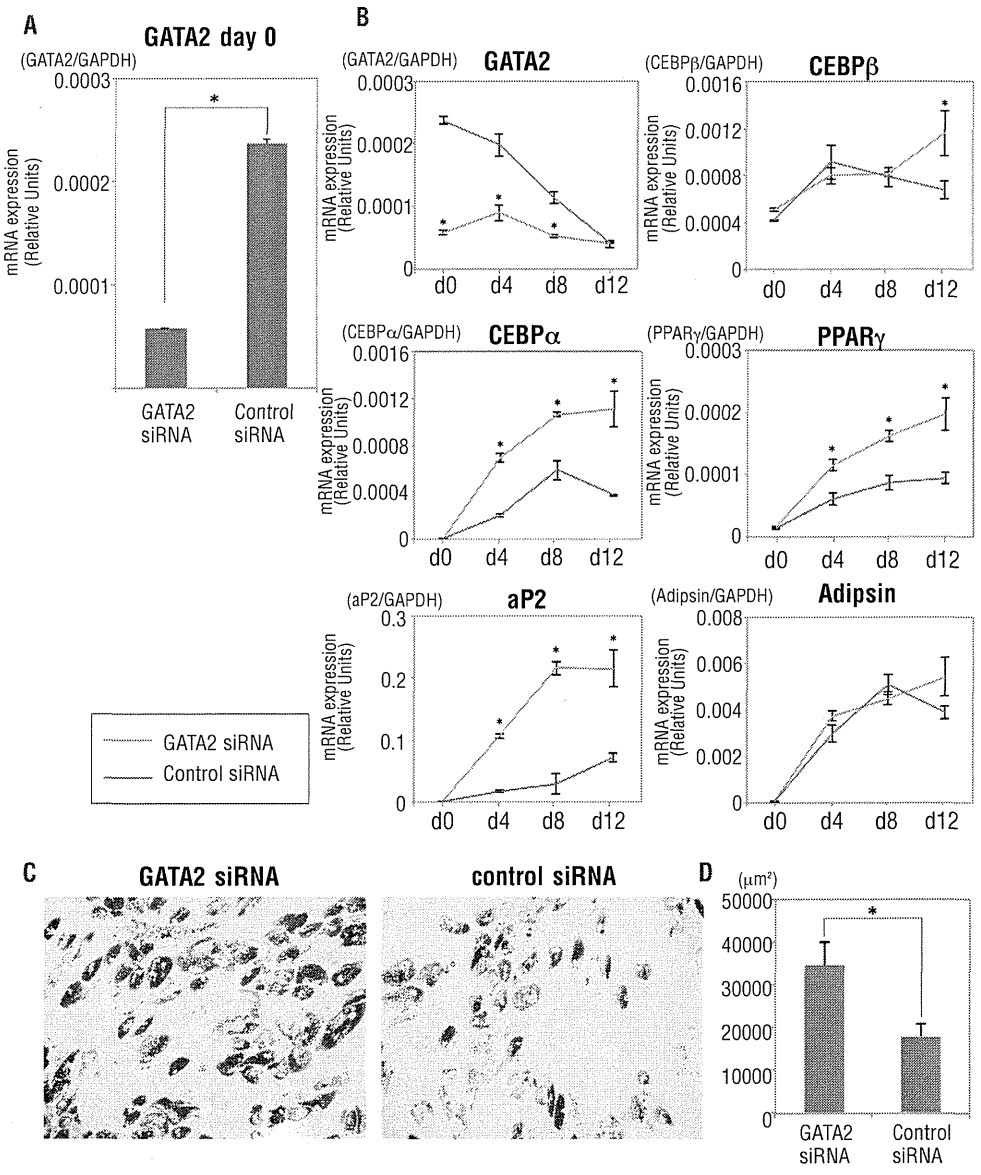

Figure 2. Effects of GATA2 knockdown on the differentiation of human MSC into adipocytes. GATA2 expression was suppressed in human BM-MSC by transfecting them with a human GATA2-siRNA, and the cells were induced to differentiate into the adipocyte lineage for up to 12 days. The data are representative of three independent BM-MSC lines. (A, B) Quantitative RT-PCR analysis for GATA2 expression on day 0 (A) and adipocyte-specific genes during adipocyte differentiation (B). The expression of each target gene relative to that of *GAPDH* was calculated. (C, D) Oil Red O staining (C) and the area of mature adipocytes (D). The data are expressed as mean ± SD (n=3). *$P<0.05$.

ENPP1, which regulate osteoblastic differentiation (Table 1).[31] In contrast, and unexpectedly, adipocyte-related genes were not detected. Gene ontology analysis revealed significant enrichment of genes related to "cell cycle" (P=8.6x10^{-11}) and "protein modification" (P=2.6 x10^{-3}; Table 2).

As described above, we identified decreased expression of various cell cycle regulatory genes after GATA2 knockdown. Previous studies of hematopoietic cells have suggested that GATA2 expression varies during the cell cycle and that GATA2 regulates cell-cycle regulators.[32,33] We, therefore, evaluated whether the cell cycle was altered in BM-MSC in which GATA2 expression was inhibited. The number of cells present in G1/G0 was significantly increased when GATA2 expression was decreased (Figure 4), which was due to the significantly increased proportion of cells in the G1 phase (*Online Supplementary Figure S4*). We further confirmed that cell proliferation was decreased by decreased GATA2 expression (Figure 5). These results suggest that GATA2 has an important role in BM-MSC proliferation by regulating cell-cycle regulators.

Reduced hematopoietic support of human bone marrow mesenchymal stem cells by GATA2 knockdown

Although BM-MSC differentiate into various cell types that form the hematopoietic microenvironment, BM-MSC themselves can support HSC.[34] To determine whether the ability of BM-MSC to support HSC was compromised by decreasing GATA2 expression levels, we co-cultured cord blood-derived CD34-positive cells with BM-MSC that were transfected with control or GATA2 siRNA. After co-culture of CD34-positive cells with the BM-MSC, the HSC fraction was isolated using the gating strategy of the International Society of Hematotherapy and Graft Engineering (ISHAGE) (Figure 6A).[35,36] The frequency of CD34-positive cells on day

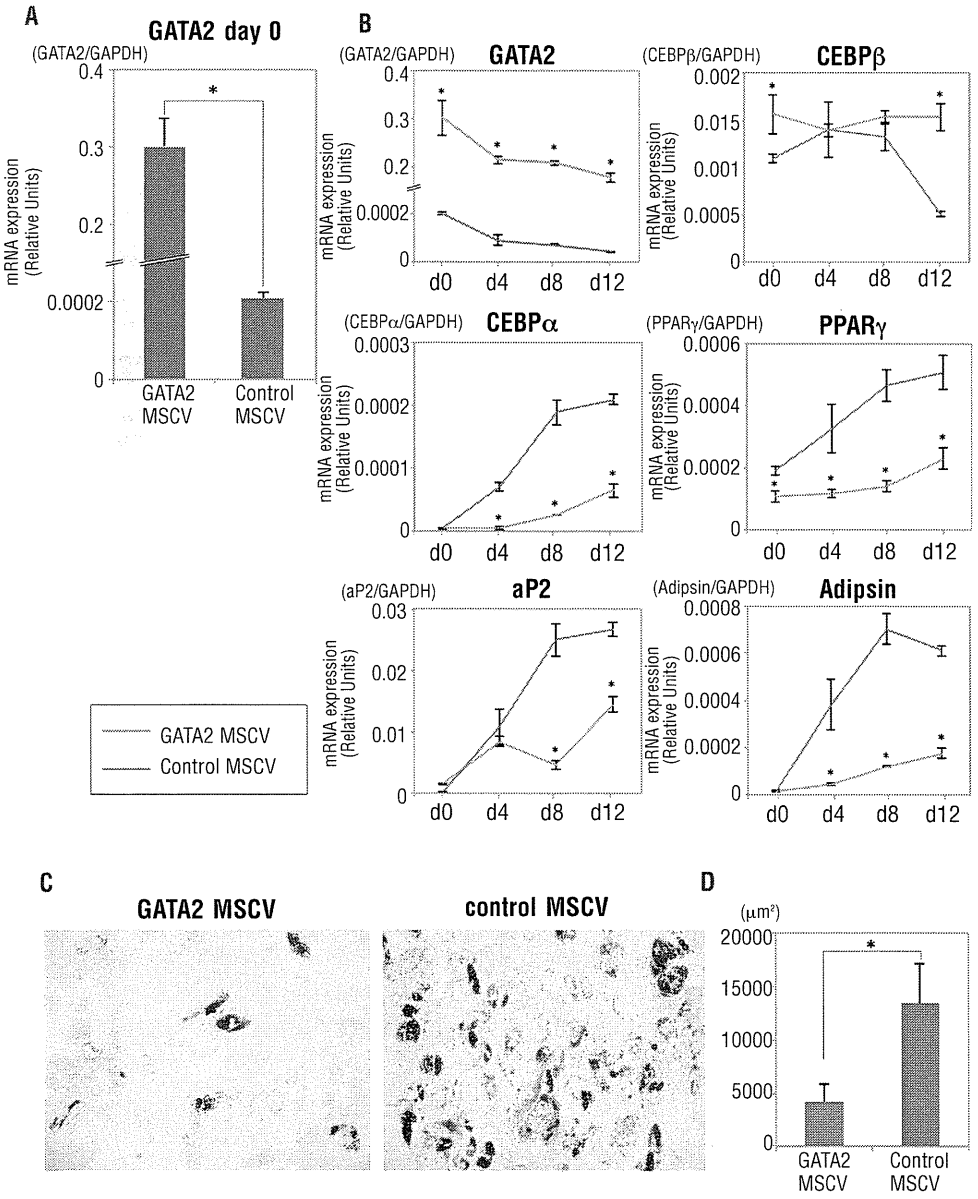

Figure 3. Effect of GATA2 overexpression on the differentiation of human MSC into adipocytes. GATA2 was overexpressed in human MSC using the MSCV retroviral vector system, and the cells were induced to differentiate into the adipocyte lineage for up to 12 days. The data are representative of three independent BM-MSC lines. (A, B) Quantitative RT-PCR analysis for GATA2 expression on day 0 (A) and adipocyte-specific genes during adipocyte differentiation (B). The expression of each target gene relative to that of *GAPDH* was calculated. *P<0.05. (C, D) Oil Red O staining (C) and the area of mature adipocytes (D). The data are expressed as mean ± SD (n=3). *P<0.05.

Table 1. List of GATA2-regulated genes in human BM-MSC.

Upregulated		Downregulated			
Fold change	Gene symbol	Fold change	Gene symbol	Fold change	Gene symbol
5.57	*SLC40A1*	0.19	*PTMA*	0.39	*LOC100506248*
5.09	*CACNA2D3*	0.22	*PGK1*	0.39	*KIF14*
4.58	*SLC16A6*	0.23	*ENPP1*	0.39	*LRRFIP1*
4.32	*IGF1*	0.24	*HJURP*	0.39	*MGAT1*
4.25	*CRYGS*	0.25	*STC1*	0.39	*TERF2IP*
3.83	*LOC100506119*	0.26	*CCNA2*	0.39	*MLF1IP*
3.74	*EGR3*	0.27	*CEP55*	0.39	*WHSC1*
3.61	*GPX3*	0.27	*AURKA*	0.39	*SQRDL*
3.41	*BEX1*	0.28	*MCM10*	0.40	*TMOD2*
3.39	*IL8*	0.28	*TOP2A*	0.40	*PRC1*
3.25	*MEGF10*	0.28	*ACAT1*	0.40	*BIRC5*
3.23	*IGFBP5*	0.29	*NSF*	0.40	*ARL5A*
3.18	*CHIC1*	0.29	*CDC6*	0.40	*CCNB1*
3.10	*GRIA1*	0.29	*CRIPT*	0.40	*RPL36*
3.04	*PTBP2*	0.29	*CNIH4*	0.40	*FANCI*
3.03	*TECPR2*	0.29	*AP2M1*	0.40	*CD44*
3.01	*NRG1*	0.29	*DTL*	0.40	*CCNE2*
2.99	*SLC44A1*	0.29	*ARG2*	0.41	*PFKFB4*
2.98	*FLRT3*	0.29	*KIF3B*	0.41	*LAMB1*
2.96	*PRL*	0.30	*ZHX1*	0.41	*PRIM1*
2.94	*LPAR6*	0.30	*C11orf82*	0.41	*PTBP1*
2.92	*C3AR1*	0.30	*PRELID1*	0.41	*DYNLT3*
2.85	*PTPRD*	0.30	*CPS1*	0.41	*SLC30A5*
2.84	*MAMDC2*	0.30	*DEPDC1*	0.42	*PRKAR2A*
2.76	*CHST15*	0.31	*TPX2*	0.42	*PRPS1*
2.75	*ZNF302*	0.31	*SPC25*	0.42	*TMPO*
2.74	*NKX3-2*	0.31	*HIST1H4A*	0.42	*MON1B*
2.69	*TPM1*	0.31	*SOCS2*	0.42	*NUF2*
2.69	*GRIA3*	0.32	*CDC20*	0.42	*OIP5*
2.67	*NOV*	0.32	*PLK4*	0.42	*DKFZP434I0714*
2.65	*EPHA5*	0.32	*GINS2*	0.42	*TGOLN2*
2.63	*TPM2*	0.32	*KIF11*	0.42	*KIF15*
2.62	*LCTL*	0.32	*C19orf10*	0.42	*RACGAP1*
2.62	*CDKN1C*	0.33	*CENPI*	0.42	*NADK*
2.60	*ADRA2A*	0.33	*HELLS*	0.42	*GCNT1*
2.60	*PDGFD*	0.33	*ROCK2*	0.43	*MTMR4*
2.60	*FNDC4*	0.33	*TMED10*	0.43	*CEBPG*
2.59	*TNPO1*	0.33	*CEP128*	0.43	*CDCA7L*
2.58	*CNTNAP3*	0.33	*CAND1*	0.43	*GTSE1*
2.58	*DEPTOR*	0.33	*SHCBP1*	0.43	*KIF4A*
2.56	*LINC00086*	0.33	*HSPA9*	0.43	*GGCX*
2.55	*SFRP1*	0.33	*C2orf18*	0.43	*TUG1*
2.55	*C12orf76*	0.33	*PXDN*	0.43	*CDT1*
2.54	*AOX1*	0.33	*ASPM*	0.43	*RNF41*
2.53	*EFHC2*	0.33	*PBK*	0.43	*CENPF*
2.52	*GDPD1*	0.33	*APOBEC3G*	0.43	*RPA1*
2.51	*LOC100653132*	0.34	*STX12*	0.43	*FOXM1*
2.51	*FAM135A*	0.34	*LRRFIP1*	0.44	*RBM45*
2.50	*SGCD*	0.34	*HMMR*	0.44	*SLC39A6*
2.48	*MTHFD2L*	0.34	*NCAPG*	0.44	*FGFR1OP2*
2.48	*ABCA8*	0.34	*RRM2*	0.44	*LEPREL1*
2.47	*KIAA0226L*	0.34	*NEK2*	0.44	*MKI67*
2.47	*NR2F1*	0.34	*FAM176B*	0.44	*HMGB2*
2.47	*CEP19*	0.35	*PRR11*	0.44	*PDE8A*
2.44	*PTPN22*	0.35	*BUB1*	0.44	*IRAK1*
2.43	*PDLIM7*	0.35	*CDCA3*	0.44	*PLEKHA3*
2.42	*PDK4*	0.35	*CDCA2*	0.44	*RFC3*
2.41	*EGR1*	0.36	*DYNC1LI2*	0.44	*CCNB2*
2.39	*SPON1*	0.36	*RAD51AP1*	0.44	*ZNF395*
2.38	*SIPA1L2*	0.36	*SPTLC1*	0.44	*CD164*
2.38	*HLA-DRA*	0.36	*UBE2C*	0.44	*TTK*
2.36	*COL24A1*	0.36	*ATG3*	0.44	*TK1*
2.34	*NME5*	0.36	*G3BP2*	0.44	*XYLT1*
2.34	*TTN*	0.36	*BUB1B*	0.44	*UHRF1*
2.33	*ACVR2A*	0.36	*CCBE1*	0.44	*NCOR1*
2.33	*LOC100505971*	0.36	*DPM2*	0.45	*CCDC50*
2.29	*ABCC3*	0.36	*FBN2*	0.45	*ATL3*
2.28	*MYL12A*	0.36	*MAD2L1*	0.45	*CIB1*
2.25	*KIAA0895*	0.37	*DNAJC30*	0.45	*PRDX6*
2.25	*EIF5A2*	0.37	*CASC5*	0.45	*SGTB*
2.24	*NCALD*	0.37	*WDR76*	0.46	*NT5E*
2.22	*HS2ST1*	0.37	*NUSAP1*	0.46	*ADAMTS5*
2.22	*MMP16*	0.37	*ELL2*	0.46	*CDKN3*
2.21	*CTSC*	0.37	*RAB30*	0.46	*AMIGO3*
2.20	*MED28*	0.37	*FAM54A*	0.46	*SNX12*
2.20	*SEPP1*	0.37	*KIF20A*	0.46	*UBLCP1*
2.17	*AR*	0.37	*SYDE1*	0.47	*VAPA*
2.17	*AKR1C3*	0.37	*SCOC*	0.47	*DPY19L3*
2.16	*LINC00340*	0.37	*KIF2C*	0.47	*LOC153546*
2.15	*ANKRD46*	0.37	*DLGAP5*	0.47	*DHX40*
2.14	*ANKRD1*	0.38	*CENPE*	0.47	*CD47*
2.14	*VPS36*	0.38	*PRICKLE4*	0.47	*BARD1*
2.13	*TRIB1*	0.38	*BCAP29*	0.47	*TRAF3*
2.13	*TMEM100*	0.38	*ARNTL2*	0.47	*P2RX4*
2.12	*JUN*	0.38	*EIF4EBP1*	0.48	*PARD6G*
2.11	*GBP1*	0.38	*NDC80*	0.48	*CKAP4*
2.11	*TBC1D19*	0.38	*C14orf1*	0.48	*RAP1GDS1*
2.07	*QPCT*	0.39	*ANLN*	0.48	*LMTK2*
2.05	*DRAM1*	0.39	*CDC25C*	0.48	*GPR107*
2.03	*CAPN3*	0.39	*ARL6IP1*	0.48	*IDS*
		0.39	*SGOL2*	0.49	*GATA2*
		0.39	*DEPDC1B*	0.49	*PRKD1*
		0.39	*WISP1*	0.49	*ABHD6*
		0.39	*CDK1*	0.49	*CHEK1*
		0.39	*MPV17L2*		

Genes showing >2-fold differentiation based on the average of two independent profiling analyses are listed.

7 tended to decrease upon co-culturing with BM-MSC with GATA2 knockdown, but this was not statistically significant (Figure 6B). Subsequently, we assessed the colony-forming capacity of CD34-positive cells after culture with each siRNA-treated BM-MSC. As shown in Figure 6C-E, the total number of colonies was significantly lower when the CD34-positive cells were cultured with BM-MSC transfected with the GATA2-siRNA. To compare the effects with a more advanced stage of adipocyte differentiation, we conducted the same series of analyses based on BM-MSC-derived adipocytes, demonstrating that HSC frequency and colony formation were decreased by GATA2 knockdown (Figure 7). In brief, our data suggest that the decrease of GATA2 expression in BM-MSC decreased the cells' ability to support the hematopoietic microenvironment.

As noted, GATA2 expression in CD34-positive cells is significantly decreased in patients with aplastic anemia by an unknown mechanism.[19,20] Because cytokines such as transforming growth factor-β,[37] interferon-γ,[37] tumor necrosis factor-α,[38,39] IL-6,[39] IL-17A,[39] and IL-1β[40,41] may be involved in the pathogenesis of aplastic anemia, we evaluated whether the addition of these cytokines may accelerate adipocyte differentiation. Unexpectedly, adipocyte differentiation was suppressed by these cytokines, except for IL-6 (*Online Supplementary Figure S5A-F*). In addition, the suppression of adipocyte differentiation did not always correlate with the changes of GATA2 expression level, nor *AP2* expression (i.e. tumor necrosis factor-α and IL-6), possibly because these cytokines might affect *AP2* expression level and adipocyte differentiation independently of GATA2. Next, we assessed the effect of bone morphogenic protein (BMP)-4, because a previous study demonstrated that BMP4 regulates GATA2 expression in embryonic stem cells.[42] As shown in *Online Supplementary Figure S5G*, BMP4 suppressed adipocyte differentiation and significantly induced GATA2, suggesting that BMP4 could be one of the factors involved in the regulation of GATA2 in BM-MSC.

Table 2. Gene ontology analysis of GATA2-regulated genes in human BM-MSC.

Biological process	Count	P value
Upregulated		
Signal transduction	24	2.50E-02
Developmental processes	18	1.30E-02
Cell communication	11	4.40E-02
Cell proliferation and differentiation	9	8.90E-02
Mesoderm development	7	4.20E-02
Muscle contraction	5	1.10E-02
Muscle development	4	2.80E-02
Extracellular matrix protein-mediated signaling	3	3.50E-02
Downregulated		
Cell cycle	40	1.40E-15
Protein modification	21	4.90E-03
Cell proliferation and differentiation	17	2.90E-02
Mitosis	17	2.60E-07
Protein phosphorylation	14	8.90E-03
Cell cycle control	12	1.80E-03
DNA metabolism	8	3.70E-02
General vesicle transport	7	3.50E-02
DNA replication	7	1.60E-03
Chromosome segregation	7	6.60E-04
Molecular function	**Count**	***P* value**
Upregulated		
Signaling molecule	8	5.20E-02
Extracellular matrix	5	7.80E-02
Growth factor	4	1.60E-02
Extracellular matrix glycoprotein	3	6.90E-02
Glutamate receptor	2	8.80E-02
Downregulated		
Kinase	16	1.10E-03
Cytoskeletal protein	14	3.50E-02
Protein kinase	12	8.00E-03
Microtubule family cytoskeletal protein	12	6.50E-06
Microtubule binding motor protein	8	1.60E-06
Non-receptor serine/threonine protein kinase	7	5.40E-02
Kinase modulator	5	6.30E-02
Transcription cofactor	5	6.00E-02
Kinase activator	4	1.80E-02

Genes showing >2-fold differentiation after GATA2 knockdown were analyzed.

Discussion

The balance between proliferation and differentiation of MSC may be tightly regulated by BMP, Hedgehog, and Wnt signaling pathways, among others.[3,43-54] BMP2 and BMP4 promote adipocyte differentiation.[47] Noggin inhibits BMP signaling and promotes osteogenic differentiation.[43] In addition, Hedgehog and Wnt signaling pathways inhibit adipocyte differentiation but promote osteoblastic differentiation.[44-48] Efforts to identify the regulatory mechanisms that control the differentiation of BM-MSC into adipocytes/osteoblasts may lead to the development of new clinical applications in the fields of regenerative medicine and tissue engineering and enhance our understanding of hematopoiesis, since BM-MSC are the primary sources of the hematopoietic microenvironment.[1]

Although GATA2 may play an important role in regulating adipocyte differentiation from a mouse preadipocytic cell line,[16-18] its role in regulating human BM-MSC differentiation is unknown. In the present study, we revealed that knockdown and overexpression of GATA2 accelerated and

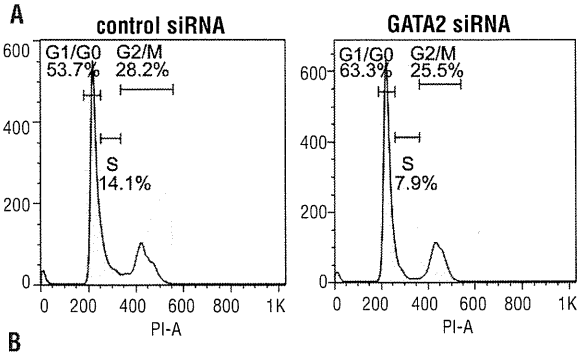

	G0/G1 stage (%)	S stage (%)	G2/M stage (%)
control siRNA	58.3 ± 7.4	10.9 ± 3.9	26.4 ± 4.8
GATA2 siRNA	65.0 ± 5.4	6.8 ± 2.2	25.3 ± 3.5

Figure 4. Increase of G1/G0 phase cells with decreased GATA2 expression in BM-MSC. (A) Representative cell-cycle profile in human BM-MSC treated with control or anti-GATA-2 siRNA, based on propidium iodide staining. (B) Percentage of cells in each stage of the cell cycle (expressed as mean ± SD, n=3).

inhibited adipocyte differentiation, respectively (Figures 2 and 3). We assumed that BM-MSC fate might be determined by the balances of multiple transcription factors, rather than solely by GATA2. For example, GATA1 and PU.1, master regulators in erythroid and granulocyte differentiation, respectively, act mutually antagonistically.[55,56] Similar antagonism has also been reported between C/EBPα and PU.1 during neutrophil differentiation.[57,58] Furthermore, in murine MSC, the propensity for differentiation toward osteoblasts or adipocytes was affected by various factors including *Maf*, *Runx2*, *Cebpb* and *Pparg*.[59,60] Nevertheless, our data clearly demonstrate that GATA2 could be one of the important factors that determine immaturity and differentiation toward adipocytes in BM-MSC.

We have demonstrated that GATA2 knockdown in BM-MSC increased the number of cells in G0/G1 (Figure 4, *Online Supplementary Figure S4*), with significant downregulation of cell cycle regulators such as *CHEK1*, *CCNB1*, *CCNB2*, *GTSE1*, and *CDC20* (Table 1). GATA2 expression oscillates during the cell cycle such that expression is high in the S phase but low in G1/S and M phases.[32] Moreover,

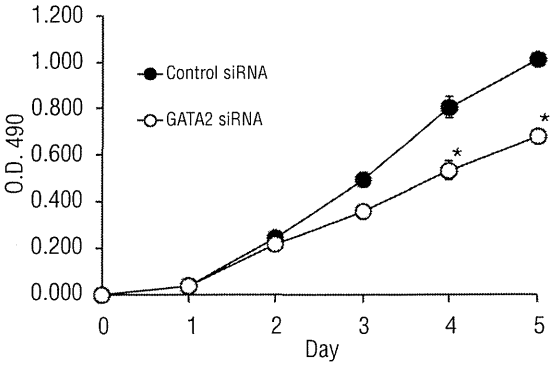

Figure 5. Effect of GATA2 knockdown on the proliferation of human BM-MSC. GATA2 expression was suppressed in human BM-MSC by transfecting them with a human GATA2-siRNA, and the cells were further cultured in the medium for 5 days. The number of viable cells was determined every 24 h by a colorimetric method. The data are expressed as mean ± SD (n=4). *P<0.05.

A

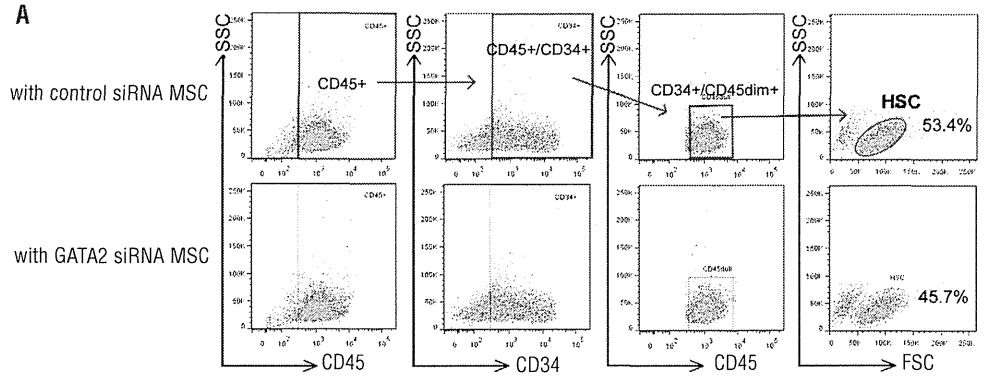

B

	with control siRNA MSC	with GATA2 siRNA MSC
HSC (%)	38.7±13.1	33.4±11.9

C

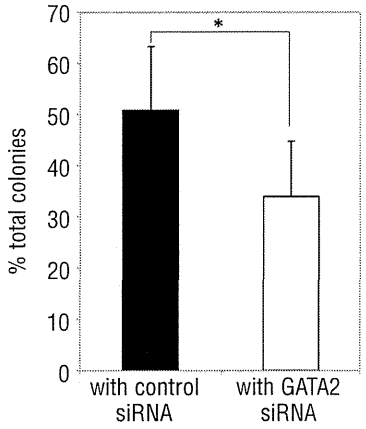

D

	BFU-E	CFU-G	CFU-M	CFU-GM	CFU-GEMM
with control siRNA MSC	14.8 ± 3.1	16.8 ± 4.3	12.0 ± 3.3	6.7 ± 5.0	1.0 ± 0.9
with GATA2 siRNA MSC	9.7 ± 4.5*	15.0 ± 2.0	8.8 ± 4.0	4.5 ± 3.7	0.2 ± 0.4

E

Figure 6. Reduced hematopoietic support of human BM-MSC by GATA2 knockdown. (A) Representative flow cytometry data to demonstrate the strategy for isolating the HSC fraction based on the ISHAGE gating strategy.[35,36] (B) The average frequency of the HSC fraction after co-culture with control or GATA2-knockdowned BM-MSC (mean ± SD, n=3). (C-E) The number of total colonies (C), each colony type (D) and representative image of colony formation (E) are shown (mean ± SD, n=3, for C and D). *P<0.05.

A

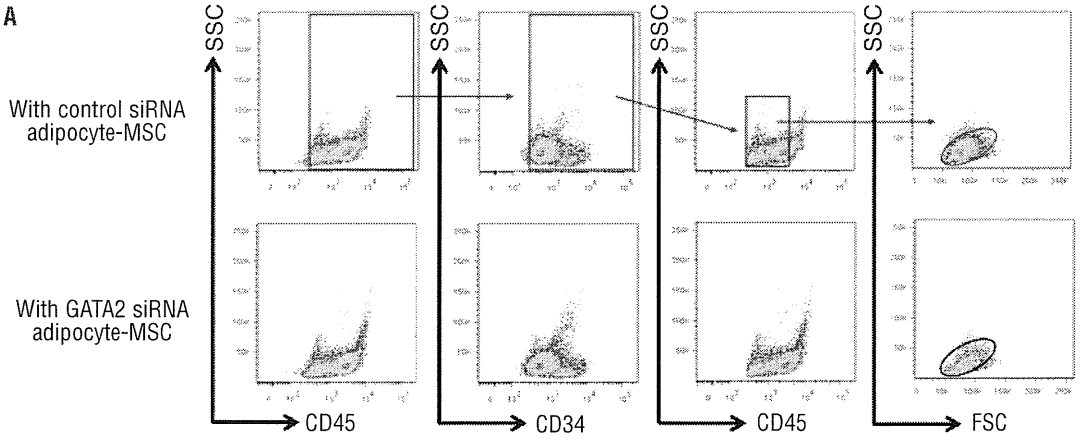

B

	with control siRNA adipocyte MSC	with GATA2 siRNA adipocyte MSC
HSC (%)	67.1 ± 4.8	37.3 ± 4.8

C

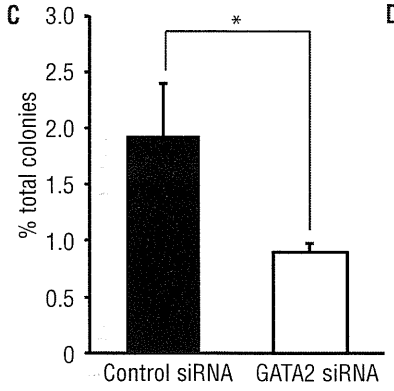

D

	BFU-E	CFU-G	CFU-M	CFU-GM	CFU-GEMM
with control siRNA	4.7 ± 4.1	4.0 ± 1.4	6.7 ± 1.2	3.3 ± 0.5	0.7 ± 0.9
with GATA2 siRNA	2.0 ± 1.6	1.7 ± 0.9	3.0 ± 0.8	1.7 ± 0.9	0.7 ± 0.5

Figure 7. Reduced hematopoietic support of human BM-MSC by GATA2 knockdown. Human BM-MSC were differentiated into adipocytes (6 days) on the day of adipocyte differentiation and subsequently, co-cultured with CD34-positive cells. (A) Representative flow cytometry data for isolating the HSC fraction based on the ISHAGE gating strategy.[35,36] (B) The average frequency of the HSC fraction after co-culture with control or GATA2-knockdowned BM-MSC differentiated into adipocytes (adipocyte-MSC) (mean ± SD, n=3). (C-D) The number of total colonies (C) and each colony type (D) are shown (mean ± SD, n=3, for C and D). *P<0.05.

GATA2 regulates cell cycle regulators, including CCND3, CDK4, and CDK6,[33] suggesting that GATA2 contributes to the regulation of the HSC pool within the bone marrow. We, therefore, conclude that GATA2-mediated cell cycle regulation occurs in BM-MSC. Recent evidence suggests that adipocyte differentiation is triggered during the G1 phase when progenitor cells are exposed to adipogenic stimuli such as insulin, insulin-like growth factor 1, dexamethasone, and cyclic AMP.[61,62] Furthermore, considering our finding that GATA2 knockdown in BM-MSC increased the number of G1 phase cells (Figure 4, *Online Supplementary Figure S4*), the susceptibility to adipogenic stimuli may have been augmented by GATA2 knockdown, leading to accelerated adipocyte differentiation.

We have also demonstrated that GATA2 expression in HSC is lower in patients with aplastic anemia and leads to decreased *HOXB4* expression,[19,20] which would contribute to the reduction in the size of the HSC pool.[26] Furthermore, GATA2 expression is also lower in BM-MSC derived from patients with aplastic anemia.[13] In the present study, we demonstrated that decreased GATA2 expression in BM-MSC accelerated adipocyte differentiation. Thus, decreased GATA2 expression by HSC and BM-MSC may lead to decreased number of HSC as well as fatty marrow change, which is a characteristic feature of aplastic anemia.

In addition to the accelerated adipocyte differentiation from BM-MSC by GATA2 knockdown (Figure 2), we further demonstrated that GATA2-knockdowned BM-MSC compromised colony-forming capacity based on co-culture with CD34-positive cells (Figure 6). Although the molecular mechanism responsible for this effect is unknown, decreased expression of cell adhesion molecules such as *LAMB1*, *CD44*, and *FBN2* (Table 1) may be involved in impaired HSC maintenance. *LAMB1* encodes laminin β1, which is expressed in the hematopoietic microenvironment, and contributes to the regulation of hematopoiesis.[63] Furthermore, CD44 promotes the homing process between HSC and the hematopoietic niche through hyaluronic acid, which serves as a ligand.[64,65] Thus, GATA2 downregulation in patients with aplastic anemia may result in a decrease of extracellular matrix, similar to the functions of LAMB1 and CD44, resulting in impaired HSC support.

Immunosuppressive therapy is effective in 75% of cases of aplastic anemia, suggesting that immunological injury plays a role in the pathogenesis of aplastic anemia.[66] However, in our study, the addition of various cytokines did not accelerate adipocyte differentiation or decrease GATA2 expression (*Online Supplementary Figure S5*), suggesting that

transforming growth factor-β, interferon-γ, tumor necrosis factor-α, IL-6 and IL-17A and IL-1β might not be involved in the regulation of GATA2 expression in BM-MSC. We included BMP4 in our analysis because this protein regulates GATA2 expression.[42] As expected, we demonstrated that BMP4 induced GATA2 expression, suggesting that BMP4 may affect GATA2 expression in BM-MSC (*Online Supplementary Figure S5G*). However, we observed that the addition of BMP4 suppressed adipocyte differentiation, unlike the results of another study on preadipocytic C3H10T1/2 cell lines.[47] We suggest that this difference may be attributed, in part, to the concentration of BMP4 used here. Nevertheless, in addition to BMP signaling, several factors, such as the Wnt signaling pathway, regulate GATA2 expression.[67] Further analyses are, therefore, required to elucidate the pathogenesis of aplastic anemia.

In conclusion, our findings support the hypothesis that GATA2 plays an important role in regulating the differentiation potential of BM-MSC and contributes to hematopoietic supporting capacity. Therefore, in bone marrow, GATA2 is not only involved in the generation and/or maintenance of HSC, but also in regulating the hematopoietic microenvironment. Identifying the regulatory mechanism of GATA2 in HSC and BM-MSC may lead to the development of novel therapeutic approaches for bone marrow failure syndromes.

Acknowledgments

We thank the staff of the Department of Hematology and Rheumatology for helpful discussions and members of the Biomedical Research Core of Tohoku University School of Medicine and Biomedical Research Unit of Tohoku University Hospital for support. We thank Drs. T Kitamura, M Kurokawa and S Camper for providing the PLAT-F retroviral vector, iCre-producing MP34 cell line and GATA2 conditional knockout mice, respectively. All animal experiments were conducted at the Institute for Animal Experimentation, Tohoku University Graduate School of Medicine.

Authorship and Disclosures

Information on authorship, contributions, and financial & other disclosures was provided by the authors and is available with the online version of this article at www.haematologica.org.

References

1. Frenette PS, Pinho S, Lucas D, Scheiermann C. Mesenchymal stem cell: keystone of the hematopoietic stem cell niche and a stepping-stone for regenerative medicine. Annu Rev Immunol. 2013;31:285–316.
2. Naveiras O, Nardi V, Wenzel PL, Hauschka PV, Fahey F, Daley GQ. Bone-marrow adipocytes as negative regulators of the haematopoietic microenvironment. Nature. 2009;460(7252):259–63.
3. Nishikawa M, Ozawa K, Tojo A, Yoshikubo T, Okano A, Tani K, et al. Changes in hematopoiesis-supporting ability of C3H10T1/2mouse embryo fibroblasts during differentiation. Blood. 1993;81(5): 1184–92.
4. Calvi LM, Adams GB, Weibrecht KW, Weber JM, Olson DP, Knight MC, et al. Osteoblastic cells regulate the haematopoietic stem cell niche. Nature. 2003;425(6960): 841–6.
5. Pittenger MF, Mackay AM, Beck SC, Jaiswal RK, Douglas R, Mosca JD, et al. Multilineage potential of adult human mesenchymal stem cells. Science. 1999;284(5411):143–7.
6. Lowell BB. PPARgamma: an essential regulator of adipogenesis and modulator of fat cell function. Cell. 1999;99(3):239–42.
7. Tang QQ, Lane MD. Adipogenesis: from stem cell to adipocyte. Annu Rev Biochem. 2012;81:715–36.
8. Cao Z, Umek RM, McKnight SL. Regulated expression of three C/EBP isoforms during adipose conversion of 3T3-L1 cells. Genes Dev. 1991;5(9):1538–52.
9. Rangwala SM, Lazar MA. Transcriptional control of adipogenesis. Annu Rev Nutr. 2000;20:535–59.
10. Tsai FY, Keller G, Kuo FC, Weiss M, Chen J, Rosenblatt M, et al. An early haematopoietic defect in mice lacking the transcription factor GATA-2. Nature. 1994;371(6494): 221–6.
11. Harigae H. GATA transcription factors and hematological diseases. Tohoku J Exp Med. 2006;210(1):1–9.
12. Bresnick EH, Lee HY, Fujiwara T, Johnson KD, Keles S. GATA switches as developmental drivers. J Biol Chem. 2010;285(41): 31087–93.
13. Xu Y, Takahashi Y, Wang Y, Hama A, Nishio N, Muramatsu H, et al. Downregulation of GATA-2 and overexpression of adipogenic gene-PPARgamma in mesenchymal stem cells from patients with aplastic anemia. Exp Hematol. 2009;37(12):1393–9.
14. Tsai FY, Orkin SH. Transcription factor GATA-2 is required for proliferation/survival of early hematopoietic cells and mast cell formation, but not for erythroid and myeloid terminal differentiation. Blood. 1997;89(10):3636–43.
15. Zhou Y, Yamamoto M, Engel JD. GATA2 is required for the generation of V2 interneurons. Development. 2000;127(17):3829–38.
16. Tong Q, Dalgin G, Xu H, Ting CN, Leiden JM, Hotamisligil GS. Function of GATA transcription factors in preadipocyte– adipocyte transition. Science. 2000;290 (5489):134–8.
17. Okitsu Y, Takahashi S, Minegishi N, Kameoka J, Kaku M, Yamamoto M, et al. Regulation of adipocyte differentiation of bone marrow stromal cells by transcription factor GATA-2. Biochem Biophys Res Commun. 2007;364(2):383–7.
18. Tong Q, Tsai J, Tan G, Dalgin G, Hotamisligil GS. Interaction between GATA and the C/EBP family of transcription factors is critical in GATA-mediated suppression of adipocyte differentiation. Mol Cell Biol. 2005;25(2):706–15.
19. Fujimaki S, Harigae H, Sugawara T, Takasawa N, Sasaki T, Kaku M. Decreased expression of transcription factor GATA-2 in haematopoietic stem cells in patients with aplastic anaemia. Br J Haematol. 2001;113 (1):52–7.
20. Zeng W, Chen G, Kajigaya S, Nunez O, Charrow A, Billings EM, et al. Gene expression profiling in CD34 cells to identify differences between aplastic anemia patients and healthy volunteers. Blood. 2004;103(1): 325–32.
21. Charles MA, Saunders TL, Wood WM, Owens K, Parlow AF, Camper SA, et al. Pituitary-specific Gata2 knockout: effects on gonadotrope and thyrotrope function. Mol Endocrinol. 2006;20(6):1366–77.
22. Goyama S, Yamamoto G, Shimabe M, Sato T, Ichikawa M, Ogawa S, et al. Evi-1 is a critical regulator for hematopoietic stem cells and transformed leukemic cells. Cell Stem Cell. 2008;3(2):207–20.
23. Solchaga LA, Penick K, Porter JD, Goldberg VM, Caplan AI, Welter JF. FGF-2 enhances the mitotic and chondrogenic potentials of human adult bone marrow-derived mesenchymal stem cells. J Cell Physiol. 2005;203(2):398–409.
24. Auletta JJ, Zale EA, Welter JF, Solchaga LA. Fibroblast growth factor-2 enhances expansion of human bone marrow-derived mesenchymal stromal cells without diminishing their immunosuppressive potential. Stem Cells Int. 2011;2011:235176.
25. Bianchi G, Banfi A, Mastrogiacomo M, Notaro R, Luzzatto L, Cancedda R, Quarto R. Ex vivo enrichment of mesenchymal cell progenitors by fibroblast growth factor 2. Exp Cell Res. 2003;287(1):98–105.
26. Fujiwara T, Yokoyama H, Okitsu Y, Kamata M, Fukuhara N, Onishi Y, et al. Gene expression profiling identifies HOXB4 as a direct downstream target of GATA-2 in human CD34+ hematopoietic cells. PLoS One. 2012;7(9):e40959.
27. Sekine R, Kitamura T, Tsuji T, Tojo A. Efficient retroviral transduction of human B-lymphoid and myeloid progenitors: marked inhibition of their growth by the Pax5 transgene. Int J Hematol. 2008;87(4):351–62.
28. Sung JH, Yang HM, Park JB, Choi GS, Joh JW, Kwon CH, et al. Isolation and characterization of mouse mesenchymal stem cells. Transplant Proc. 2008;40(8):2649–54.
29. Pittenger MF, Mackay AM, Beck SC, Jaiswal RK, Douglas R, Mosca JD, et al. Multilineage potential of adult human mesenchymal stem cells. Science. 1999;284(5411):143–7.
30. Boiret N, Rapatel C, Veyrat-Masson R, Guillouard L, Guérin JJ, Pigeon P, et al. Characterization of nonexpanded mesenchymal progenitor cells from normal adult human bone marrow. Exp Hematol. 2005;33(2):219–25.
31. Nam HK, Liu J, Li Y, Kragor A, Hatch NE. Ectonucleotide pyrophosphatase/phosphodiesterase-1 (ENPP1) protein regulates osteoblast differentiation. J Biol Chem.

2011;286(45):39059–71.
32. Koga S, Yamaguchi N, Abe T, Minegishi M, Tsuchiya S, Yamamoto M, Minegishi N. Cell-cycle-dependent oscillation of GATA2 expression in hematopoietic cells. Blood. 2007;109(10):4200–8.
33. Tipping AJ, Pina C, Castor A, Hong D, Rodrigues NP, Lazzari L, et al. High GATA-2 expression inhibits human hematopoietic stem and progenitor cell function by effects on cell cycle. Blood. 2009;113(12):2661–72.
34. Ding L, Morrison SJ. Haematopoietic stem cells and early lymphoid progenitors occupy distinct bone marrow niches. Nature. 2013;495(7440):231–5.
35. Sutherland DR, Anderson L, Keeney M, Nayar R, Chin-Yee I. The ISHAGE guidelines for CD34+ cell determination by flow cytometry. International Society of Hematotherapy and Graft Engineering. J Hematother. 1996;5(3):213–26.
36. Brocklebank AM, Sparrow RL. Enumeration of CD34+ cells in cord blood: a variation on a single-platform flow cytometric method based on the ISHAGE gating strategy. Cytometry. 2001;46(4):254–61.
37. Serio B, Selleri C, Maciejewski JP. Impact of immunogenetic polymorphisms in bone marrow failure syndromes. Mini Rev Med Chem. 2011;11(6):544–52.
38. Feng X, Young NS. Cytokine signature profiles in acquired aplastic anemia and myelodysplastic syndromes. Haematologica. 2011;96(4):602–6.
39. Gu Y, Hu X, Liu C, Qv X, Xu C. Interleukin (IL)-17 promotes macrophages to produce IL-8, IL-6 and tumour necrosis factor-alpha in aplastic anaemia. Br J Haematol. 2008;142(1):109–14.
40. Hirayama Y, Kohgo Y, Matsunaga T, Ohi S, Sakamaki S, Niitsu Y. Cytokine mRNA expression of bone marrow stromal cells from patients with aplastic anaemia and myelodysplastic syndrome. Br J Haematol. 1993;85(4):676–83.
41. Ibáñez A, Río P, Casado JA, Bueren JA, Fernández-Luna JL, Pipaón C. Elevated levels of IL-1beta in Fanconi anaemia group A patients due to a constitutively active phosphoinositide 3-kinase-Akt pathway are capable of promoting tumour cell proliferation. Biochem J. 2009;422(1):161–70.
42. Lugus JJ, Chung YS, Mills JC, Kim SI, Grass J, Kyba M, et al. GATA2 functions at multiple steps in hemangioblast development and differentiation. Development. 2007;134(2):393–405.
43. Rifas L. The role of noggin in human mesenchymal stem cell differentiation. J Cell Biochem. 2007;100(4):824–34.
44. Ross SE, Hemati N, Longo KA, Bennett CN, Lucas PC. Inhibition of adipogenesis by Wnt signaling. Science. 2000;289(5481):950–3.
45. Bowers RR, Lane MD. Wnt signaling and adipocyte lineage commitment. Cell Cycle. 2008;7(9):1191–6.
46. Bennett CN, Longo KA, Wright WS, Suva LJ, Lane TF, Hankenson KD, et al. Regulation of osteoblastogenesis and bone mass by Wnt10b. Proc Natl Acad Sci USA. 2005;102(9):3324–9.
47. Zehentner BK, Leser U, Burtscher H. BMP-2 and sonic hedgehog have contrary effects on adipocyte-like differentiation of C3H10T1/2 cells. DNA Cell Biol. 2000;19(5):275–81.
48. Spinella-Jaegle S, Rawadi G, Kawai S, Gallea S, Faucheu C, Mollat P, et al. Sonic hedgehog increases the commitment of pluripotent mesenchymal cells into the osteoblastic lineage and abolishes adipocytic differentiation. J Cell Sci. 2001;114(Pt11):2085–94.
49. van der Horst G, Farih-Sips H, Löwik CW, Karperien M. Multiple mechanisms are involved in inhibition of osteoblast differentiation by PTHrP and PTH in KS483 cells. J Bone Miner Res. 2005;20(12):2233–44.
50. Isenmann S, Arthur A, Zannettino AC, Turner JL, Shi S, Glackin CA, et al. TWIST family of basic helix-loop-helix transcription factors mediate human mesenchymal stem cell growth and commitment. Stem Cells. 2009;27(10):2457–68.
51. Xu Y, Zhou YL, Erickson RL, Macdougald OA, Snead ML. Physical dissection of the CCAAT/enhancer-binding protein alpha in regulating the mouse amelogenin gene. Biochem Biophys Res Commun. 2007;354 (1): 56–61.
52. Tang QQ, Lane MD. Activation and centromeric localization of CCAAT/enhancer binding proteins during the mitotic clonal expansion of adipocyte differentiation. Genes Dev. 1999;13(17):2231–41.
53. Korenjak M, Brehm A. E2F-Rb complexes regulating transcription of genes important for differentiation and development. Curr Opin Genet Dev. 2005;15(5):520–7.
54. Thomas DM, Carty SA, Piscopo DM, Lee JS, Wang WF, Forrester WC, et al. The retinoblastoma protein acts as a transcriptional coactivator required for osteogenic differentiation. Mol Cell. 2001;8(2):303–16.
55. Zhang P, Behre G, Pan J, Iwama A, Wara-Aswapati N, Radomska HS, et al. Negative cross-talk between hematopoietic regulators: GATA proteins repress PU.1. Proc Natl Acad Sci USA. 1999;96(15):8705–10.
56. Nerlov C, Querfurth E, Kulessa H, Graf T. GATA-1 interacts with the myeloid PU.1 transcription factor and represses PU.1-dependent transcription. Blood. 2000;95(8):2543–51.
57. Reddy VA, Iwama A, Iotzova G, Schulz M, Elsasser A, Vangala RK, et al. Granulocyte inducer C/EBPalpha inactivates the myeloid master regulator PU.1: possible role in lineage commitment decisions. Blood. 2002;100(2):483–90.
58. Dahl R, Walsh JC, Lancki D, Laslo P, Iyer SR, Singh H, et al. Regulation of macrophage and neutrophil cell fates by the PU.1:C/EBPalpha ratio and granulocyte colony-stimulating factor. Nat Immunol. 2003;4(10):1029–36.
59. Nishikawa K, Nakashima T, Takeda S, Isogai M, Hamada M, Kimura A, et al. Maf promotes osteoblast differentiation in mice by mediating the age-related switch in mesenchymal cell differentiation. J Clin Invest. 2010;120(10):3455–65.
60. Sun H, Kim JK, Mortensen R, Mutyaba LP, Hankenson KD, Krebsbach PH. Osteoblast-targeted suppression of PPARγ increases osteogenesis through activation of mTOR signaling. Stem Cells. 2013;31(10):2183–92.
61. Lee Y, Bae EJ. Inhibition of mitotic clonal expansion mediates fisetin-exerted prevention of adipocyte differentiation in 3T3-L1 cells. Arch Pharm Res. 2013;36(11):1377–84.
62. MacDougald OA, Lane MD. Transcriptional regulation of gene expression during adipocyte differentiation. Annu Rev Biochem. 1995;64:345–73.
63. Siler U, Seiffert M, Puch S, Richards A, Torok-Storb B, Müller CA, et al. Characterization and functional analysis of laminin isoforms in human bone marrow. Blood. 2000;96(13):4194–203.
64. Avigdor A, Goichberg P, Shivtiel S, Dar A, Peled A, Samira S, et al. CD44 and hyaluronic acid cooperate with SDF-1 in the trafficking of human CD34+ stem/progenitor cells to bone marrow. Blood. 2004;103(8):2981–9.
65. Malfuson JV, Boutin L, Clay D, Thépenier C, Desterke C, Torossian F, et al. SP/drug efflux functionality of hematopoietic progenitors is controlled by mesenchymal niche through VLA-4/CD44 axis. Leukemia. 2013;28(4):853-64.
66. Young NS, Scheinberg P, Calado RT. Aplastic anemia. Curr Opin Hematol. 2008;15(3):162–8.
67. Trompouki E, Bowman TV, Lawton LN, Fan ZP, Wu DC, DiBiase A, et al. Lineage regulators direct BMP and Wnt pathways to cell-specific programs during differentiation and regeneration. Cell. 2011;147(3):577–89.

tapraid4/zgb-jolb/zgb-jolb/zgb00414/zgb6061d14z | xppws | S=1 | 12/10/13 | 5:55 | Art: 5A0513-250 | Input-BW

JLB

Article

Simple diagnosis of *STAT1* gain-of-function alleles in patients with chronic mucocutaneous candidiasis

Yoko Mizoguchi,[*,1] *Miyuki Tsumura,*[*,1] *Satoshi Okada,*[*,†] *Osamu Hirata,*[*] *Shizuko Minegishi,*[‡] *Kohsuke Imai,*[§] *Nobuyuki Hyakuna,*[‖] *Hideki Muramatsu,*[¶] *Seiji Kojima,*[¶] *Yusuke Ozaki,*[#] *Takehide Imai,*[#] *Sachiyo Takeda,*[#] *Tetsuya Okazaki,*[#] *Tsuyoshi Ito,*[**] *Shin'ichiro Yasunaga,*[††] *Yoshihiro Takihara,*[††] *Vanessa L. Bryant,*[†] *Xiao-Fei Kong,*[†] *Sophie Cypowyj,*[†] *Stéphanie Boisson-Dupuis,*[†,‡‡] *Anne Puel,*[‡‡] *Jean-Laurent Casanova,*[†,‡‡] *Tomohiro Morio,*[§] *and Masao Kobayashi*[*,2]

[*]Department of Pediatrics, Hiroshima University Graduate School of Biomedical and Health Sciences, Japan; [†]St. Giles Laboratory of Human Genetics of Infectious Diseases, The Rockefeller University, New York, New York, USA; [‡]Division of Molecular Medicine, Institute for Genome Research, The University of Tokushima, Japan; [§]Department of Pediatrics and Developmental Biology, Graduate School of Medical and Dental Sciences, Tokyo Medical and Dental University, Japan; [‖]Center of Bone Marrow Transplantation, Faculty of Medicine, University of the Ryukyus, Okinawa, Japan; [¶]Department of Pediatrics, Nagoya University Graduate School of Medicine, Japan; [#]Department of Pediatrics, Nippon Medical School, Tokyo, Japan; [**]Department of Pediatrics, Toyohashi Municipal Hospital, Japan; [††]Department of Stem Cell Biology, Research Institute for Radiation Biology and Medicine, Hiroshima University, Japan; and [‡‡]Laboratory of Human Genetics of Infectious Diseases, Necker Branch, Necker Medical School, INSERM U980, and University Paris Descartes, Paris, France

RECEIVED MAY 5, 2013; REVISED NOVEMBER 13, 2013; ACCEPTED DECEMBER 2, 2013. DOI: 10.1189/jlb.0513250

ABSTRACT

CMCD is a rare congenital disorder characterized by persistent or recurrent skin, nail, and mucosal membrane infections caused by *Candida albicans*. Heterozygous GOF *STAT1* mutations have been shown to confer AD CMCD as a result of impaired dephosphorylation of STAT1. We aimed to identify and characterize *STAT1* mutations in CMCD patients and to develop a simple diagnostic assay of CMCD. Genetic analysis of *STAT1* was performed in patients and their relatives. The mutations identified were characterized by immunoblot and reporter assay using transient gene expression experiments. Patients' leukocytes are investigated by flow cytometry and immunoblot. Six GOF mutations were identified, three of which are reported for the first time, that affect the CCD and DBD of *STAT1* in two sporadic and four multiplex cases in 10 CMCD patients from Japan. Two of the 10 patients presented with clinical symptoms atypical to CMCD, including other fungal and viral infections, and three patients developed bronchiectasis. Immunoblot analyses of patients' leukocytes showed abnormally high levels of pSTAT1 following IFN-γ stimulation. Based on this finding, we performed a flow cytometry-based functional analysis of *STAT1* GOF alleles using IFN-γ stimulation and the tyrosine kinase inhibitor, staurosporine. The higher levels of pSTAT1 observed in primary CD14$^+$ cells from patients compared with control cells persisted and were amplified by the presence of staurosporine. We developed a flow cytometry-based STAT1 functional screening method that would greatly facilitate the diagnosis of CMCD patients with GOF STAT1 mutations.

***J. Leukoc. Biol.* 95: 000–000; 2014.**

Introduction

Patients with CMCD suffer from persistent or recurrent skin, nail, and mucosal membrane infections caused by *C. albicans* [1, 2]. CMCD is also observed in patients with primary immunodeficiencies, such as T cell deficiencies, AD HIES, AR IL-12p40 deficiency, AR IL-12Rβ1 deficiency, and AR APS-1 [3–6]. Patients with AD HIES have very low levels of IL-17A- and IL-22-producing T cells as a result of an impairment of STAT3-mediated responses [7–10]. The numbers of IL-17A- and IL-22-producing T cells are also low in patients with IL-12p40 and IL-12Rβ1 deficiencies but to a lesser extent than in patients with AD HIES [8]. Patients with APS-1 develop high titers of

Abbreviations: AD=autosomal-dominant, APS-1=autoimmune polyendocrinopathy type 1 syndrome, AR=autosomal-recessive, CCD=coiled-coil domain, CMCD=chronic mucocutaneous candidiasis disease, DBD=DNA-binding domain, GAF=γ-activating factor, GAS=γ-activated sequence, GOF=gain-of-function, HIES=hyper-IgE syndrome, IRF=IFN regulatory factor, ISG=IFN-stimulated gene, ISRE=IFN-stimulated response element, MFI=mean fluorescence intensity, MSMD=mycobacterial disease, pSTAT1=phosphorylated STAT1, qPCR=quantitative PCR

The online version of this paper, found at www.jleukbio.org, includes supplemental information.

1. These authors contributed equally to this manuscript.

2. Correspondence: Dept. of Pediatrics, Hiroshima University Graduate School of Biomedical Sciences, 1-2-3 Kasumi, Minami-ku, Hiroshima 734–8551, Japan. E-mail: masak@hiroshima-u.ac.jp AQ

neutralizing autoantibodies against IL-17A, IL-17F, and/or IL-22 [11, 12]. These findings suggest that human IL-17A, IL-17F, and/or IL-22 may be essential for mucocutaneous immunity to *C. albicans* [6]. This hypothesis led to the discovery of AR IL-17RA deficiency and AD IL-17F deficiency as genetic etiologies of CMCD without other severe infectious diseases (isolated CMCD) [13]. Thus, inborn errors of IL-17 immunity can underlie CMCD [14–17]. However, no genetic etiology has yet been identified for the vast majority of patients with CMCD.

Heterozygous mutations affecting the CCD of *STAT1* were identified recently by next-generation sequencing in patients with AD CMCD [18, 19]. A heterozygous T385M mutation, affecting the DBD of STAT1, was then discovered [20]. These mutations led to increases in Tyr701 pSTAT1, GAF DNA-binding ability, and IFN GAS transcription activity in response to IFN-γ, IFN-α, and IL-27 [18, 20, 21]. Surprisingly, there, GOF STAT1 alleles account for approximately one-half of patients with CMCD in previous studies (ref. [18] and unpublished results). The underlying molecular mechanism was deciphered using inhibitors of kinases and phosphatases and was shown to result from the impaired nuclear dephosphorylation of STAT1 [18]. We report here six GOF *STAT1* mutations, three of which have never been described before, in two sporadic and four familial cases from four Japanese families with AD CMCD. We found that $CD14^+$ monocytes from the patients displayed persistent pSTAT1 in response to IFN-γ and in the presence of the tyrosine kinase inhibitor staurosporine. Based on this observation, we developed a flow cytometry-based simple and rapid STAT1 functional screening method to facilitate the diagnosis of CMCD patients with GOF STAT1 mutations.

MATERIALS AND METHODS

Patients

Clinical information is summarized in **Table 1**. STAT1 mutations identified in patients and familial segregation of *STAT1* mutations are shown in **Fig. 1B**.

Kindred A (L354M/WT). The proband (A-I-1: P1) is a 45-year-old man who has suffered from recurrent tinea unguium and otitis media since the age of 3 years. He also had several episodes of herpes virus infection, resulting in herpes simplex keratitis, dermatitis herpetiformis, and shingles during his childhood. At the age of 22, he experienced cryptococcal meningitis; he was diagnosed with hypothyroidism and placed on levofloxacin treatment. This patient also suffers from bronchiectasis and irritable bowel syndrome. His son is 7 years old (A-II-2) and suffers from recurrent oral aphthous lesions due to *C. albicans*. He has experienced no clinical episode suggestive of host susceptibility to viral or invasive fungal infection. At the age of 6 years, he was diagnosed with hypothyroidism and began treatment with levothyroxine. Both P1 and his son (A-II-2) have been found to have persistent, slightly high liver enzyme levels.

Kindred B (M202V/WT). The patient (B-II-1: P2) is a 34-year-old man with recurrent stomatitis as a result of *C. albicans* since infancy. He was diagnosed with CMCD at the age of 5 years. Oral itraconazole treatment was initiated at the age of 18 years, but this patient still suffers from persistent tinea unguium and oral candidiasis. He has suffered from bronchopneumonia more than twice yearly since his 20s. Sputum cultures were systematically negative for bacteria, but the bronchopneumonia seemed to respond to treatment with levofloxacin and cefotiam. No hypothyroidism has been detected.

Kindred C (A267V/WT). The proband (C-I-2: P3) is a 10-year-old boy. He developed onychomycosis at the age of 18 months and was treated with antifungal drugs for 6 months. He has presented no *Candida* infections since this episode. P3 had vascular purpura at the age of 6 years but does not have hypothyroidism. His mother (C-II-1) is 44 years old. She developed onychomycosis at the age of 1, vaginal candidiasis and tinea pedis at the age of 20, and recurrent oral candidiasis in her 30s, at which time, she

TABLE 1. Summary of 10 Patients with CMCD from Six Kindred

Patients	*STAT1* mutation	Fungal infections	Viral infection	Other complication
A-I-1	L354M	recurrent tinea unguium, cryptococcal meningitis	recurrent herpes virus infection	recurrent otiti media, bronchiectasis, irritable bowel syndrome, hypothyroidism, persistent, slightly elevated liver enzyme
A-II-2	L354M	recurrent oral aphthous as a result of *C. albicans*		hypothyroidism, persistent, slightly elevated liver enzyme
B-II-1	M202V	persistent tinea unguium, recurrent stomatitis as a result of *C. albicans*		bronchopneumonia
C-I-2	A267V	onychomycosis, tinea pedis, oral, esophageal, vaginal candidiasis		bronchiectasis, antiparietal cell antibody-positive megaloblastic anemia, hypothyroidism, persistent, slightly elevated liver enzyme
C-II-1	A267V	onychomycosis		vascular purpura
D-I-2	R274Q	recurrent oral and esophageal candidiasis, persistent skin candidiasis		
D-II-2	R274Q	oral candidiasis		
E-II-1	P329L	oral thrush		
E-II-2	P329L	recurrent oral thrush		pure red blood cell aplasia, autoimmune hemolytic anemia
F-II-1	M390T	recurrent oral and skin candidiasis	severe chicken-pox, chronic EBV infection	low serum IgG2 levels, bronchiectasis, mild hypothyroidism, recurrent severe diarrhea, recurrent otitis media, elevated liver enzyme

tapraid4/zgb-jolb/zgb-jolb/zgb00414/zgb6061d14z | xppws | S=1 | 12/10/13 | 5:55 | Art: 5A0513-250 | Input-BW

COLOR

AQ: 3

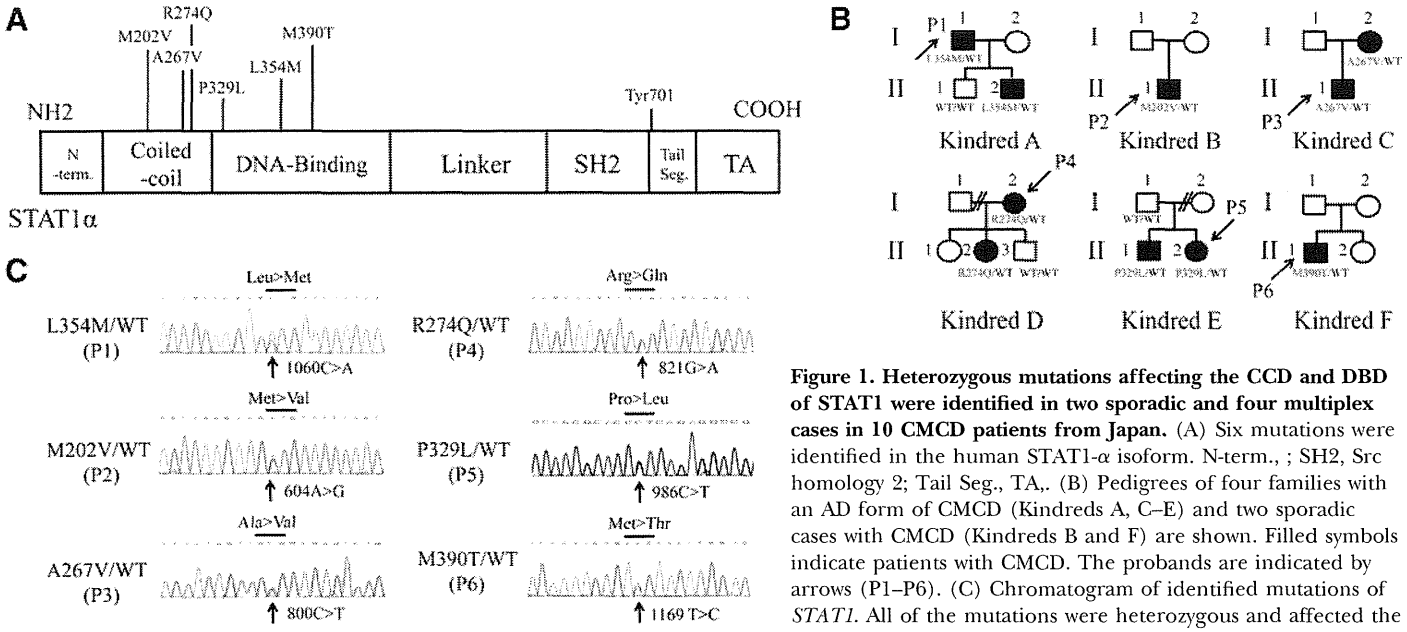

Figure 1. Heterozygous mutations affecting the CCD and DBD of STAT1 were identified in two sporadic and four multiplex cases in 10 CMCD patients from Japan. (A) Six mutations were identified in the human STAT1-α isoform. N-term., ; SH2, Src homology 2; Tail Seg., TA,. (B) Pedigrees of four families with an AD form of CMCD (Kindreds A, C–E) and two sporadic cases with CMCD (Kindreds B and F) are shown. Filled symbols indicate patients with CMCD. The probands are indicated by arrows (P1–P6). (C) Chromatogram of identified mutations of *STAT1*. All of the mutations were heterozygous and affected the CCD or DBD of STAT1.

was also diagnosed with bronchiectasis. At the age of 42 years, balloon dilatation was performed to relieve esophageal obstruction as a result of esophageal candidiasis. This patient also has hypothyroidism and antiparietal cell antibody-positive megaloblastic anemia. She was diagnosed with persistent slightly high liver enzyme levels.

Kindred D (R274Q/WT). The proband (D-I-2: P4) is a 32-year-old woman. She developed oral and cutaneous candidiasis at the age of 1 year and pneumonia with pleural effusion at the age of 10 years. The disease-causing pathogen was not identified, but the patient's symptoms improved rapidly after the initiation of antifungal treatments. Oral fluconazole treatment was introduced after this episode. However, the patient suffered from persistent skin candidiasis and recurrent esophageal candidiasis. Her second daughter (D-II-2) also suffers from oral candidiasis. This familial case was reported in a previous manuscript (Kindred H in ref. [18]).

Kindred E (P329L/WT). The proband (E-II-1: P5) is a 16-year-old girl who has suffered from recurrent oral thrush since infancy. At the age of 14 years, she displayed pure red blood cell aplasia and autoimmune hemolytic anemia, which responded to treatment with steroid and cyclosporine A. Her older brother (E-II-2) is 17 years old and has also suffered from oral thrush. Their father had no *STAT1* mutation, and no clinical or genetic information was available for their mother.

Kindred F (M390T/WT). The patient (F-II-1: P6) is a 30-year-old man with recurrent oral candidiasis since the age of 2 years. He suffered from severe chicken-pox at the age of 1 year, which took 90 days to resolve fully. He developed pneumonia at the age of 3 years, at which point, CMCD was suspected. After this episode, he suffered from recurrent, severe diarrhea, skin and oral candidiasis, and otitis media. The candidiasis was intractable despite treatment with antifungal drugs. At the age of 14 years, this patient was found to have low serum IgG2 levels and was given Ig replacement therapy. At the age of 17 years, he developed an impairment of liver function, and elevated liver enzyme was detected in serum. He also presented recurrent fever of unknown origin. He was found to have a high titer of EBV-transformed B cells in serum (1.9×10^5 copies/ml; reference range $<1\times10^2$ copies/ml). He did not produce antibody against EBV nuclear antigen, which neutralizes EBV, during the clinical course of his illness, and chronic EBV infection was therefore suspected. This patient also has bronchiectasis and very mild hypothyroidism that does not require treatment. His parents and his younger sister do not present the clinical phenotype of CMCD.

Molecular genetic analysis

Genomic DNA was extracted from peripheral blood leukocytes. Complete coding exons of *STAT1* and their flanking introns were amplified by PCR and sequenced. We inserted the various alleles of *STAT1* into the pcDNA3-V5 vector [18, 22, 23]. We also generated the P329L, L354M, and M390T mutations of *STAT1* by PCR-based mutagenesis with mismatched primers. Primer sequences and PCR conditions are available on request.

Flow cytometric analysis

We assessed pSTAT1 in PBMCs from the patients. The MFI of pSTAT1 depended on the timing of the analysis. We therefore systematically assayed PBMCs, 24 h after blood collection. Mononuclear cells were suspended at a density of 10^4 cells/μl in serum-free RPMI. The cells were incubated with IFN-γ (1000 U/ml) for 15 min. They were then washed and incubated with 0.5 μM staurosporine (for 15 or 30 min for flow cytometry experiments and 15 min for immunoblot assays) in RPMI and subjected to analysis. For flow cytometry, the cells were stained simultaneously with anti-human CD3, CD19, or CD14 FITC antibody (BD PharMingen, San Diego, CA, USA) and treated with staurosporine. They were fixed and permeabilized, according to the BD Phosflow protocol (Protocol III); stained with FITC-conjugated anti-CD3, CD19, or CD14 and PE-conjugated anti-pSTAT1 (BD PharMingen) antibodies; and subjected to flow cytometric analysis. It took 6 h to perform the complete flow cytometric analysis.

Immunoblot analysis and EMSA

STAT1-null U3C fibrosarcoma cells were maintained in DMEM, supplemented with 10% FBS. The cells were harvested and replated at a density of 2.5×10^5 cells/ml in six-well culture plates. After incubation for a further 24 h, plasmid DNA (5 μg/well), carrying the WT or a mutant STAT1 allele, was introduced into the cells by calcium phosphate-mediated transfection. The transfected cells were incubated for 24 h, and 10^4 IU/ml IFN-γ was then added. The cells were incubated for a further 15 min and then subjected for EMSA and immunoblot analysis. Immunoblot analysis was performed as described previously [24]. The primary antibodies used were an anti-pSTAT1 (pY701) antibody (BD Biosciences, San Jose, CA, USA; Cell Signaling Technology, Danvers, MA, USA); an anti-STAT1 antibody (C-24; Santa Cruz Biotechnology, Santa Cruz, CA, USA); and an anti-

β-actin antibody (Sigma-Aldrich, St. Louis, MO, USA). EMSA was carried out as described previously [24]. After IFN-γ stimulation, U3C-transfected cells were subjected to nuclear extraction. We incubated 20 μg nuclear extract with ^{32}P-labeled (α-dATP) GAS (produced under control for the *FCGR1* promoter) probe for 30 min.

Luciferase reporter assay

Luciferase assays were performed as described previously [18, 22, 23]. Briefly, transfected U3C cells were stimulated with IFN-α (5000 IU/ml), IL-27 (20 mg/ml), or various concentrations of IFN-γ (1, 5, 10, 50, 100, 500, and 1000 IU/ml) for 8 h and then analyzed. The data are expressed as fold inductions with respect to unstimulated cells. Experiments were performed in triplicate.

qPCR analysis

CD14$^+$ monocytes were purified from PBMCs by magnetic sorting (BD Biosciences) and stimulated with 1000 IU/ml IFN-γ for 2 or 8 h. Then, total RNA was extracted and used for reverse transcription with random primers to generate cDNA. IRF1, CXCL9, and ISG15 mRNA levels were determined by qPCR with Taqman probes. The results were normalized with respect to the values obtained for the endogenous GAPDH cDNA.

Statistical analysis

Statistical significance was analyzed by nonparametric Mann-Whitney U-tests and variance followed by Tukey's post hoc analysis using SPSS software. For all analyses, $P < 0.05$ was considered statistically significant.

RESULTS

Identification of *STAT1* mutations

We investigated five sporadic and five familial cases of CMCD from a total of 15 patients from 10 kindreds. Heterozygous *STAT1* mutations were identified in two sporadic and four familial cases (and four additional cases were identified among affected relatives who were subsequently recruited, giving a total of 10 patients). Thus, *STAT1* mutations were commonly identified in Japanese patients with CMCD. We identified three previously unknown heterozygous mutations of *STAT1*: c.1060C > A (L354M) in P1 and his younger son (A-II-2), c.986C > T (P329L) in P5 and her elder brother (E-II-2), and c.1169T > C (M390T) in P6 (Fig. 1C). We also identified previously reported heterozygous mutations: c.604A > G (M202V) in P2 and c.800C > T (A267V) in P3 and her son (C-II-1) [18, 19]. The c.821G > A (R274Q) mutation was identified in P4 and her second daughter (D-II-2). This familial case is reported in a previous manuscript (Kindred K in ref. [18]). None of these mutations were identified in the healthy relatives tested, suggesting that clinical penetrance was complete. The newly identified mutations, P329L, L354M, and M390T, were not found in the National Center for Biotechnology Information, Ensembl, or dbSNP databases. They were also absent from 1052 controls from 52 ethnic groups in the Centre d'Etude du Polymorphisme Humain and Human Genome Diversity panels. These three mutations are thus rare variants rather than common, irrelevant polymorphisms segregating with AD CMCD.

Impairment of STAT1 Tyr701 dephosphorylation in PBMCs

Previous in vitro studies suggested that CMCD-related *STAT1* mutations impair nuclear dephosphorylation [18]. However, only few reports investigate dephosphorylation of STAT1 in primary cells from the patients ex vivo [25, 26]. We analyzed pSTAT1 protein in PBMCs from P4, P5, and two healthy controls. As shown in **Fig. 2A**, STAT1 protein levels were normal in the CMCD patients' PBMCs. The patients' cells contained some pSTAT1 in the absence of stimulation, and the levels of pSTAT1 increased strongly in response to IFN-γ stimulation, remaining high after treatment with the tyrosine kinase inhibitor staurosporine, which inhibits JAK-STAT signaling upstream of STAT1, probably as a result of impaired nuclear STAT1 dephosphorylation. The upper and lower bands correspond to STAT1α and STAT1β in the pSTAT1 blot, whereas the bands correspond to STAT1α in the STAT1 blot.

We first investigated IFN-γ-induced pSTAT1 by flow cytometry, using various subsets isolated from PBMCs from healthy controls and patients with CMCD (Supplemental Fig. 1). A high level of pSTAT1 was observed in CD14$^+$ monocytes, whereas it was not obvious in CD3$^+$ T cells or CD19$^+$ B cells. These observations were highly consistent with the data of previous studies [27–30]. Patients' cells showed a higher level of IFN-γ-induced pSTAT1 compared with healthy control. We therefore investigated STAT1 dephosphorylation focusing on CD14$^+$ monocytes. As the *STAT1* GOF mutations are thought to be associated with impairment in dephosphorylation of STAT1 [16], we used staurosporine to clarify the difference between *STAT1* WT alleles and *STAT1* GOF alleles. If the STAT1 dephosphorylation normally occurs in the nucleus, then pSTAT1 should decrease promptly following staurosporine treatment. Most of the patient blood samples were available only 24 h of transport. To control for the effect of time of blood processing on pSTAT1 and STAT1 dephosphorylation, we studied PBMCs from the same donor under two conditions: immediately after collection of blood samples or after a delay of 24 h (Supplemental Fig. 2). The level of pSTAT1 decreased in all of the conditions tested in the blood samples that were delayed. Thus, we decided to perform all assays in PBMCs, isolated and tested 24 h after blood collection. PBMCs from one patient with CMCD, carrying a WT *STAT1* allele; 14 healthy individuals; and 10 GOF *STAT1* patients—five from Kindreds A–C and five CMCD patients from another cohort carrying GOF *STAT1* mutations (nonreported cases)—were incubated with IFN-γ for 15 min. The cells were then washed and incubated with staurosporine-containing media for 15 min prior to analysis. For P1 only, we also measured pSTAT1 after 30 min of staurosporine treatment. Figure 2B shows a representative histogram comparing P1 and control. CD14$^+$ monocytes from P1 had higher levels of pSTAT1 than control cells following IFN-γ stimulation. The CD14$^+$ monocytes from the control displayed rapid STAT1 dephosphorylation, whereas pSTAT1 persisted in the patients' monocytes in the presence of staurosporine. Residual pSTAT1 was found in the cells of P1, even after 30 min of treatment with staurosporine. The summary of MFI values for pSTAT1 obtained by flow cytometry is shown in Fig. 2C. Some overlap was observed, but levels of pSTAT1, in response to IFN-γ, were significantly higher in CD14$^+$ cells from the patients than in those from the controls (*P<0.001). In the absence of stimulation, pSTAT1 levels were higher in the patients' cells than in control cells (*P<0.011).

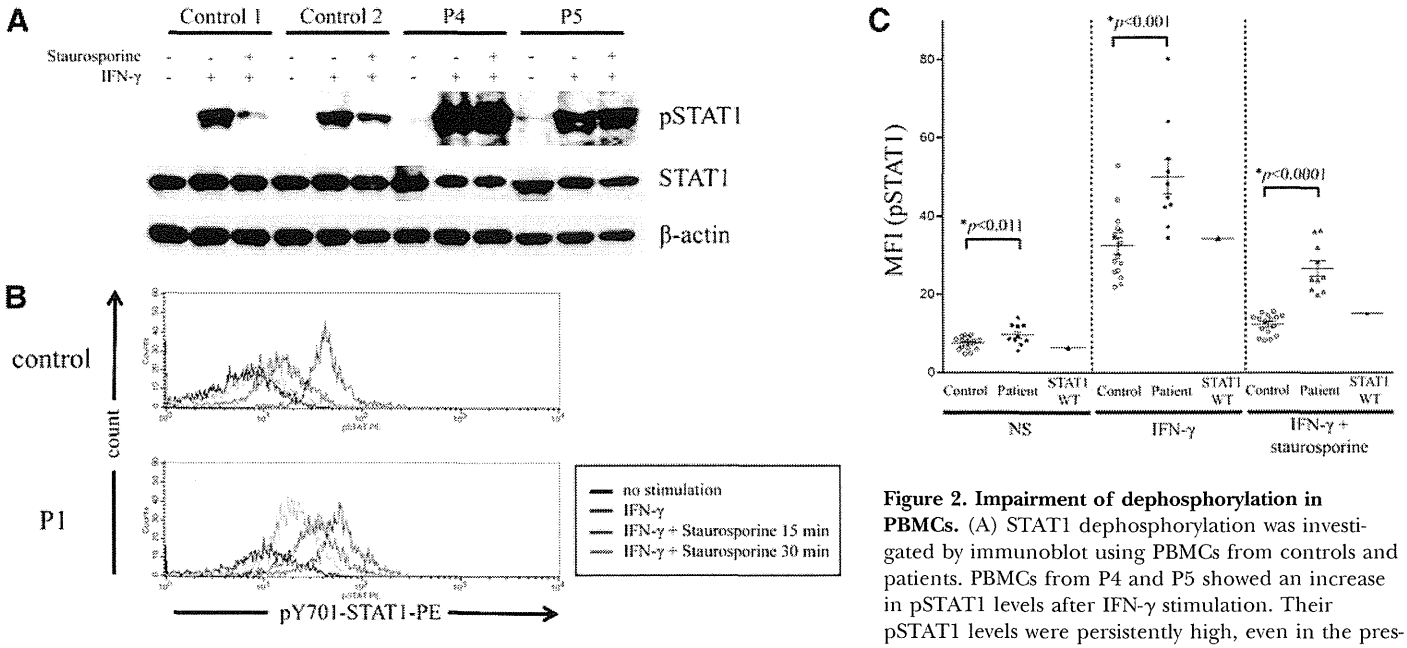

Figure 2. Impairment of dephosphorylation in PBMCs. (A) STAT1 dephosphorylation was investigated by immunoblot using PBMCs from controls and patients. PBMCs from P4 and P5 showed an increase in pSTAT1 levels after IFN-γ stimulation. Their pSTAT1 levels were persistently high, even in the presence of staurosporine. Immunoblot analysis was carried out twice to confirm the results. (B and C) PBMCs from the 10 patients, 14 healthy individuals, and one patient with CMCD, carrying a WT *STAT1* allele, were stimulated with IFN-γ and incubated in the presence of staurosporine. The cells were stained with anti-CD14 and anti-pY701 STAT1 antibodies and analyzed by flow cytometry with gating on CD14. The figures show a representative histogram of pSTAT1 intensity (B) and a summary of the MFI of pSTAT1 (C). (B) Black line, No stimulation; blue line, IFN-γ for 15 min; red and orange lines, incubation with staurosporine for 15 or 30 min, respectively, after IFN-γ stimulation.

This excess phosphorylation persisted after 15 min of treatment with staurosporine, a tyrosine kinase inhibitor (*$P<0.0001$). Moreover, in these conditions, there was no overlap in MFI of pSTAT1 between the patients and healthy controls or with a CMCD patient carrying a WT STAT1 allele. The atypical clinical signs observed in the patients did not affect the results of flow cytometric analysis. The difference in the percentage decrease in pSTAT1 levels in the presence of staurosporine between healthy controls and patients was significant too (*$P<0.02$; Supplemental Fig. 3). These results clearly indicate that the dephosphorylation process is impaired in CMCD patients. The flow cytometric analysis of pSTAT1 levels in monocytes has been established previously as a screening tool to identify IFN-γ signaling defects in patients with Mendelian susceptibility to MSMDs [31]. Taken together, this flow cytometry-based technique is likely to be useful for the rapid assessment of STAT1 function in CMCD patients.

Induction of ISGs in CD14$^+$ monocytes

We investigated the induction of ISGs in patients' cells by purifying CD14$^+$ monocytes, stimulating them with IFN-γ, and assessing the expression of the downstream ISGs *CXCL9*, *IRF1*, and *ISG15* by RT-qPCR analysis (**Fig. 3**). The induction of these three ISGs has been shown to be STAT1-dependent in previous studies [22–24, 32, 33]. CD14$^+$ monocytes from patients with CMCD (P2 and P4 and a patient carrying a R274W mutation from another cohort) showed a significantly higher induction of *CXCL9* and *IRF1* expression than did those of healthy controls. By contrast, we did not see a significant increase in the induction of ISG15 in the patients. These results suggest that the mutated *STAT1* alleles identified in CMCD patients are GOF in terms of the induction of transcription for many, but probably not all, downstream ISGs.

Increased pSTAT1 and GAF DNA-binding ability

For confirmation of the STAT1 gain-of-phosphorylation observed in primary cells from the patients, we investigated STAT1-dependent signaling pathways by transiently transfecting STAT1-null U3C fibrosarcoma cells. STAT1 protein production was normal for the CMCD-related STAT1 mutants (**Fig. 4A**). Upon IFN-γ stimulation, all of the mutant proteins displayed higher levels of pSTAT1, at least a 1.5-fold increase over WT, as determined by densitometry (Supplemental Fig. 4). As expected, phosphorylation of the MSMD-related mutant, L706S STAT1, was impaired [34]. Thus, all of the CMCD-related mutations identified resulted in a gain of phosphorylation in response to IFN-γ. Next, we assessed the DNA-binding ability of the mutant STAT1 proteins to the GAS sequence using the same transfected cells, which were subjected to immunoblot analysis (Fig. 4B). All mutants, including the three mutations identified in the DBD, displayed GOF properties, resulting in an increase of GAF binding to DNA. However, the DNA binding to GAS was abolished in the MSMD-related mutant, L706S STAT1.

Transcriptional activity of the CMCD-related STAT1 mutant protein

Transcriptional activity was studied by transfecting U3C cells with reporter plasmids and plasmids carrying the WT and/or

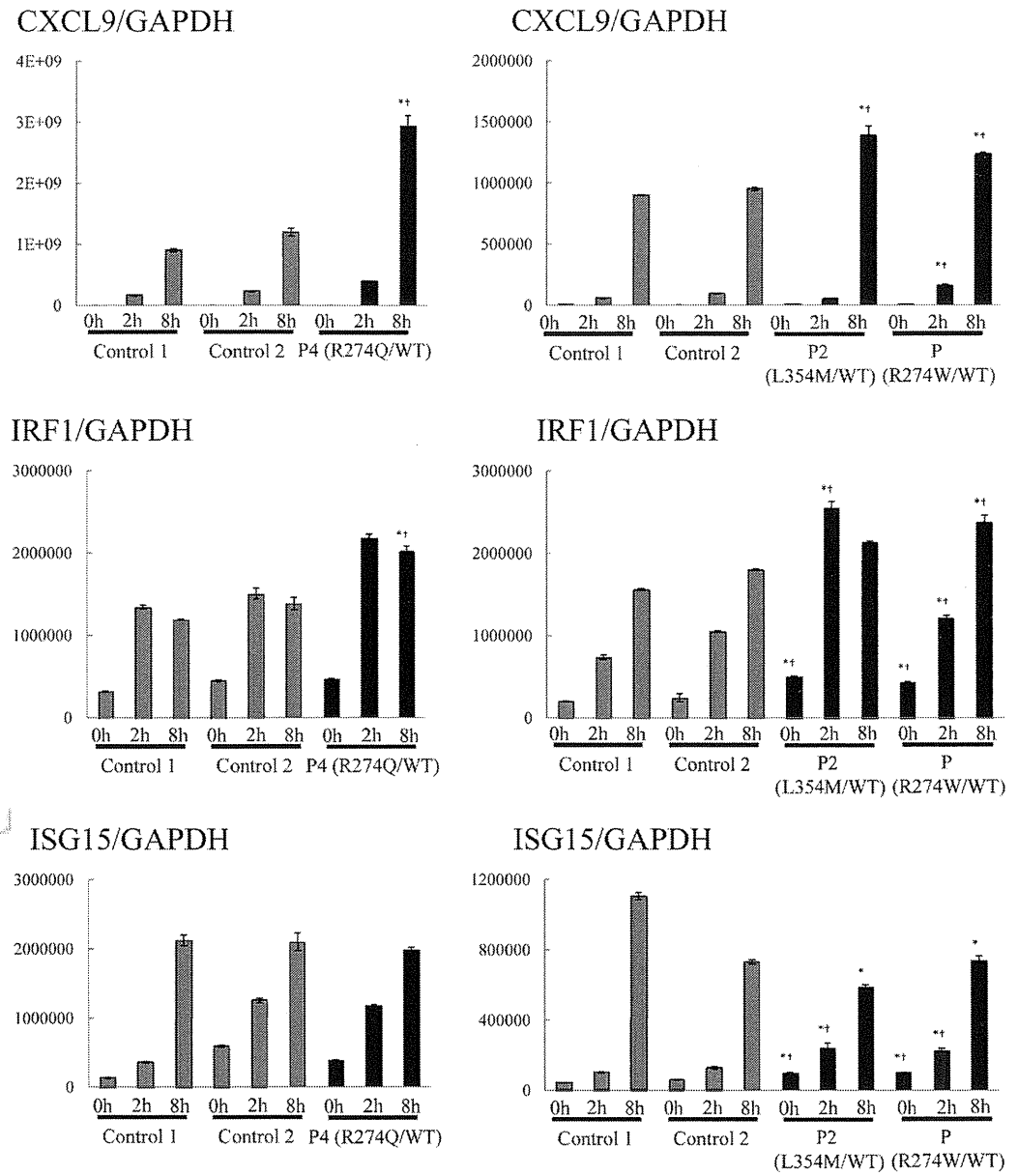

Figure 3. The induction of ISGs in CD14$^+$ monocytes. CD14$^+$ monocytes from P4 and two healthy controls were stimulated with 1000 U/ml IFN-γ (2 or 8 h), and the expression of the downstream ISGs *CXCL9*, *IRF1*, and *ISG15* was assessed by RT-qPCR. Much stronger induction of *CXCL9* and *IRF1* was observed in the patients' cells than in control cells, whereas there was no significant increase in *ISG15* induction. The expression of ISGs was normalized with respect to that of endogenous *GAPDH*. The results are representative of three independent experiments, except for the CD14$^+$ monocyte experiment (performed twice). Differences were statistically significant in the cells expressing the mutant STAT1s compared with Control 1 cells (*$P<0.05$) and Control 2 cells (†$P<0.05$).

mutant alleles of *STAT1*. The cells transfected with the CMCD-related alleles, except for M390T, had levels of GAS transcriptional activity in response to IFN-γ, more than twice those of cells transfected with the WT allele (Fig. 4C). The L706S MSMD-related *STAT1* allele abolished the transcriptional activity of GAS. The increase in GAS transcriptional activity was only slight for the M390T protein in this condition. However, the GOF became obvious when the cells were stimulated with low concentrations of IFN-γ (Fig. 4E). We also investigated IL-27-induced GAS activation (Supplemental Fig. 5) and confirmed excess GAS induction in all of the CMCD-related mutations. We then assessed ISRE transcription activity in response to IFN-α (Fig. 4D). Some positive effects on ISRE transcription activity were suspected in CMCD-related mutations, but they were not statistically significant. Thus, all of the CMCD-related mutations caused a GOF-to-GAS-mediated transcription. Moreover, the GOF was more marked at lower concentrations of IFN-γ.

DISCUSSION

In this study, *STAT1* mutations were identified with a high frequency (almost 70%) in Japanese CMCD patients; we identified heterozygous *STAT1* mutations in two of five sporadic cases and in eight of 10 cases from five multiplex kindreds. In total, we identified 10 CMCD patients with GOF *STAT1* mutations from a total of 15 diseased individuals. *STAT1* mutations were also found in ~50% of the patients with CMCD, identified in a previous study investigating large numbers of patients from numerous countries (ref. [18] and unpublished results). It remains possible that the frequency of *STAT1* mutations is